Plant Physiology Preview. Published on April 6, 2017, as DOI:10.1104/pp.17.00036

Modelling of dolichol mass spectra isotopic envelopes as a tool to monitor isoprenoid biosynthesis

Adam Jozwiak[1,#], Agata Lipko[1], Magdalena Kania[2], Witold Danikiewicz[2], Liliana Surmacz[1], Agnieszka Witek[1], Jacek Wojcik[1], Konrad Zdanowski[1,3], Cezary Pączkowski[4], Tadeusz Chojnacki[1], Jaroslaw Poznanski[1,*] and Ewa Swiezewska[1,*]

[1]Institute of Biochemistry and Biophysics, Polish Academy of Sciences, Pawinskiego 5A, 02 - 106 Warsaw, Poland

[2]Institute of Organic Chemistry, Polish Academy of Sciences, Kasprzaka 44/52, 01- 224 Warsaw, Poland

[3]Institute of Chemistry, University of Natural Sciences and Humanities, 3 Maja 54, 08-110 Siedlce, Poland

[4]Department of Plant Biochemistry, Faculty of Biology, University of Warsaw, Miecznikowa 1, 02-096 Warsaw, Poland

[#]Present address: Department of Plant and Environmental Sciences, Weizmann Institute of Science, Rehovot 7610001, Israel

[*]corresponding authors

Ewa Swiezewska,

Department of Lipid Biochemistry,

Institute of Biochemistry and Biophysics,

Polish Academy of Sciences,

Pawinskiego 5A,

02 - 106 Warsaw, Poland
fax +48225922190
phone +48225923510
e-mail ewas@ibb.waw.pl

Jaroslaw Poznanski,
Department of Biophysics,
Institute of Biochemistry and Biophysics,
Polish Academy of Sciences,
Pawinskiego 5A,
02 - 106 Warsaw, Poland
fax +48225922190
phone +48225925783
e-mail jarek@ibb.waw.pl

Abstract

The co-operation of the mevalonate (MVA) and methylerythritol phosphate (MEP) pathways, operating in parallel in plants to generate isoprenoid precursors, has been studied extensively. Elucidation of the isoprenoid metabolic pathways is indispensable for rational design of plant and microbial systems for production of industrially valuable terpenoids.

Here we describe a new method, based on numerical modeling of mass spectra of metabolically labeled dolichols (Dols), designed to quantitatively follow the co-operation of the MVA and MEP reprogrammed upon osmotic stress (sorbitol treatment). The contribution of the MEP pathway increased significantly (reaching 100%) exclusively for the dominating Dols while for long-chain Dols the relative input of the MEP and MVA pathways remained unchanged suggesting divergent site of synthesis of dominating and long-chain Dols.

Analysis of numerically modeled dolichol mass spectra is a novel method to follow modulation of the concomitant activity of isoprenoid generating pathways in plant cells, and additionally, it suggests exchange of isoprenoid intermediates between plastids and peroxisomes.

Introduction

Isopentenyl diphosphate (IPP), the building block of isoprenoids – the most numerous class of secondary metabolites - is derived in plants from two pathways operating in parallel – the cytoplasmic mevalonate (MVA) and the plastidic methylerythritol phosphate (MEP) one (Rohmer, 1999; Pulido et al., 2012). Analysis of over 130 isoprenoids has shown that in angiosperms under standard growth conditions carotenoids and chlorophyll phytyl chains on one hand and phytosterols on the other are made nearly exclusively via a single pathway (MEP and MVA, respectively), while numerous other isoprenoids, including dolichols (Skorupinska-Tudek et al., 2008), are of mixed origin (Hemmerlin et al., 2012).

The co-operation of the two pathways (often called 'cross-talk') is considered essential for plant adaptive responses to biotic and abiotic stresses. Consequently, their relative contribution to the formation of IPP is modulated and expression of particular genes of the MVA and MEP pathways is frequently correlated with stress (pathogen attack, elicitation, wounding, etc.) (Hemmerlin et al., 2012) or plant development (Opitz et al., 2014). Interestingly, the effect of stress on the regulation of the MEP-MVA balance has so far been analyzed only qualitatively.

Several methodologies have been employed to unravel the relative contribution of the MVA and MEP pathways to isoprenoids, e.g., metabolic labeling with isotopically labeled precursors (stable or radio-isotopes were used) followed by structural analysis of the product of interest or blockage either of the pathway (chemical – with pathway-specific inhibitors or genetic) followed by quantification of the isoprenoid intermediates and/or end-products. Advantages and limitations of these experimental approaches have been summarized recently (Lipko & Swiezewska, 2016).

Polyisoprenoids are composed of a few up to more than 100 isoprene units with a saturated (dolichols, Dol) or unsaturated (polyprenols) α-terminal residue (Fig. 1).

Arabidopsis hairy roots contain a complex Dol mixture comprising three groups ('families') differing in chain (Jozwiak et al., 2013). Their biosynthesis is catalyzed by *cis*-prenyltransferases (CPTs) and six out of nine putative CPT-encoding genes of Arabidopsis are expressed in roots (Surmacz and Swiezewska, 2011). Eukaryotic CPT performs sequential condensations of the isopentenyl diphosphate with an all-*trans* initiator to form a mixture of homologous polyprenyl diphosphates (PPP), which subsequently are converted to dolichols according to tissue-specific requirements (Cantagrel et al. 2010; Jozwiak et al., 2015). Structural analysis of polyisoprenoids of various species led to the conclusion that polyprenols of plant origin with a chain length within the range of 5–9 and more than 16 isoprenoid residues as well as polyprenols isolated from bacteria belong to di-*trans* structures (trivial name 'betulaprenols') suggesting that farnesyl diphosphate (FPP) serves as their all-*trans* initiator. The same type of structure, i.e. FPP-initiated biosynthesis, was found for dolichols. Polyprenols with a middle chain length (9–15 residues) represent tri-*trans* compounds (trivial name 'ficaprenols') indicating their origin from all-*trans* geranylgeranyl diphosphate (GGPP) (Swiezewska & Danikiewicz 2005).

The importance of Dol in the cell comes from the indispensable role of dolichyl phosphate as an obligate cofactor for protein glycosylation, a ubiquitous posttranslational modification found in all domains of life (Schwarz & Aebi, 2011). Glycosylation of proteins is crucial for cell functioning, since it modulates protein folding and quality control, and is a prerequisite for diverse biological recognition events (Moremenetal et al., 2012). Furthermore, based on the considerably increased accumulation of polyisoprenoids in eukaryotic cells upon aging or pathological conditions their role in cell adaptation to such conditions has been postulated too (Bergamini, 2003; Bajda et al., 2009).

Accumulation of diverse specialized metabolites, including isoprenoids, is often induced by abiotic or biotic stimuli (Sharma et al., 2013). In response to a changing

environment a specific gene expression program is activated and the plant metabolic network is reconfigured to maintain essential metabolism and to adjust to the new conditions.

In this study the novel method to quantitatively analyze the co-operation of the MEP and MVA pathways was established using numerical models of the mass spectra of metabolically labeled Dols. It allowed to follow the reorganization of the isoprenoid metabolism upon osmotic stress and suggested significantly increased contribution of the MEP pathway to Dol biosynthesis, i.e. upon the stress practically all isoprene units of the dominating Dols (Dol-14 -16) originated from the MEP pathway in contrast to control conditions where only 11 or 12 units were of the MEP origin. Conversely, the relative contribution of the MEP and MVA pathways to long Dols (n>17) was unaltered upon osmotic stress (again, 11 or 12 units from MEP pathway) suggesting a different, possibly peroxisomal, site of their biosynthesis. In a broader perspective, methodology applied here can be used to analyze the effect of various stressors on the co-operation of the MEP and MVA pathways in plant cells.

Results

Here, we describe the method to quantitatively analyze the contribution of the MEP and MVA pathways to the biosynthesis of selected isoprenoids in plant cells. Methodology employed here exemplifies the use of isotope tracing to define the metabolic pathway and, in general, such strategy is widely employed in the field of isoprenoids. It is based on metabolic labeling with isotope-labeled general (glucose) and pathway-specific (mevalonate or deoxyxylulose) precursors followed by the analysis of structure of the compound of interest. In this report meta-analysis of mass spectra of metabolically-labeled dolichols was performed - numerical simulation of the shape of their isotopic envelope. Such approach takes into account all the cationic forms of the Dol ions recorded in the spectrum (Fig. 2 and Fig. 3). Analysis of the MS spectra of Dols metabolically labeled with uniformly labeled [U-$^{13}C_6$] glucose led to quantitative estimation of the general cellular effects due to sorbitol treatment (Fig. 5 and Supplementary Fig. 3). However, to elucidate the contribution of the MEP and MVA pathways to Dol biosynthesis spectra obtained after metabolic labeling with [1-^{13}C]glucose were analyzed (Fig. 7). Application of this metabolic precursor permits differentiation of the MEP- and MVA-derived isoprene units (two or three ^{13}C atoms get incorporated, respectively, see Fig. 1B); consequently molecular ions of respective Dol are either 'lighter' or 'heavier' (MEP- or MVA-derived, respectively). Modeling of MS spectra led to quantification of the contribution of the MEP and MVA pathway (Table 2).

Dol metabolism upon osmotic stress – biochemical analysis

To optimize the experimental conditions effect of various stressors on the level and spectrum of dolichols in Arabidopsis hairy root culture was analyzed. The content of Dol in roots treated with sorbitol (0.2 to 0.5 M) increased comparing to control (Fig. 1) and their composition was modified, namely the ratio of the dominating to long-chain Dols increased upon most of the treatments tested, e.g., 5-fold in 0.3 M sorbitol (Table 1) suggesting different roles of these two Dol subgroups in cell functioning. Furthermore, sorbitol caused diverse changes in the expression of CPT-encoding genes (Fig. 1), namely expression of *CPT3*, *-6*

148 and -*7* was induced while that of *CPT1*, -*2* and -*9* was considerably reduced. Interestingly, a
149 microarray analysis (eFP Browser, http://bar.utoronto.ca/efp/cgi-bin/efpWeb.cgi) has also
150 revealed enhanced expression of *CPT3* and -*6* upon osmotic stress. The changing ratio of
151 dolichol families and the contrasting responses of different *CPT* genes in response to osmotic
152 stress suggested that at least three CPTs take part in Dol biosynthesis. Since CPT6 produces
153 shorter prenyl alcohols (Kera et al., 2012; Surmacz et al., 2014) CPT-3 and/or -7 might
154 possibly operate to synthesize dominating Dols. Moreover, out of six CPTs expressed in
155 Arabidopsis roots CPT-3 seems the most similar to the yeast Rer2 - CPT synthesizing a
156 family of Dols with Dol-16 dominating (Fig. 1). At the same time one of the stress-non-
157 responsive CPTs (CPT-1, -2 or -9) might be involved in the synthesis of long-chain Dols
158 because their accumulation is not induced by stress in Arabidopsis hairy roots. These
159 tempting suppositions, however, need experimental proofs. To analyze whether the effect of
160 sorbitol on Dol accumulation is specific the effects of oxidative agents and heavy metal salt
161 ($CdCl_2$) was elucidated in parallel (Table 1) and it was found that apart from sorbitol also
162 these abiotic stressors increased Dol accumulation. Conversely, expression pattern of *CPTs*
163 was treatment-specific (Supplementary Fig. 1 and Supplementary Fig. 2) suggesting dedicated
164 roles of individual CPTs in plant responses to different stresses and implying a role of ROS
165 signaling in dolichol generation. Analysis of the content of polyprenols (Prens), α-unsaturated
166 counterparts accompanying Dols in Arabidopsis hairy roots (Jozwiak et al., 2013), performed
167 in parallel, revealed modest decrease of their total content with the concomitant increase of
168 Dols upon sorbitol treatment (Fig. 1). Interestingly, similarly to Dols, modulation of the Pren
169 composition was noted too, namely fraction of Pren-15 -17 was considerably increased upon
170 these conditions (Table 1); since Pren-15 -17 serve as immediate substrates for polyprenol
171 reductase (PPRD) to synthesize respective Dols this observation again point out to the
172 important cellular role of dominating Dols. Accordingly, observed was mild increase of the

level of *PPRD2* mRNA (Fig. 1F), the main PPRD isoform responsible for conversion of polyprenols to dolichol in Arabidopsis seedlings (Jozwiak et al., 2015).

In contrast to the Dols, the total content of phytosterols did not change upon sorbitol treatment (Table 1).

To test the effect of osmotic stress on the MEP and MVA pathways the roots were fed either [U-$^{13}C_6$]glucose or [1-^{13}C]glucose in the absence or presence of 0.3 M sorbitol and isolated polyisoprenoids were subjected to HPLC/ESI-MS analysis (Fig. 2).

The spectra obtained were then analyzed numerically, i.e. the 'shape' of the theoretical isotopic envelope of isotopomers of each Dol-n was fitted with the experimental one.

Elucidation of Dol biosynthesis – application of mass spectrometry to analyzing [^{13}C]Dolichols

To address the possible modulatory effect of osmotic stress on the co-operation of the MVA and MEP pathways, Arabidopsis hairy roots were metabolically fed either with [U-$^{13}C_6$]glucose or [1-^{13}C]glucose in the absence or presence of 0.3 M sorbitol and isolated polyisoprenoids (Fig. 2A, inset) were subjected to HPLC/ESI-MS analysis. Careful inspection of the mass spectra of the [^{13}C]Dols revealed a complex pattern of signals (Fig. 2 and Fig. 3). The complexity of these mass spectra reflects the dispersion of the probability of formation of differentially labeled [^{13}C]Dol isotopomers/isotopologs (Skorupinska-Tudek et al., 2008). One should also note that upon MS analysis Dols form monovalent ions (z = 1), thus the recorded m/z corresponds to the mass of the ion (m) (Skorupinska-Tudek et al., 2003; Jozwiak et al., 2013). Moreover, the signal of each isotopomer (of a given m/z) in fact corresponds to various isotopologs (Dol ions containing the same number of ^{13}C atoms differently localized along the polyisoprenoid chain). Since this phenomenon was not analyzed here, the discrete isotopological structure of the MS spectrum will not be discussed further.

198 The spectra of native and metabolically labeled Dols (Fig. 2 and Fig. 3) isolated from roots
199 grown in the control and osmotic stress conditions clearly revealed that besides the $[M+Na]^+$
200 adducts identified earlier (Skorupinska-Tudek et al., 2008) also signals corresponding to
201 $[M+NH_4]^+$ were noticed, and in some runs $[M+H]^+$ or $[M+K]^+$ were also observed (Fig. 2 for
202 Dol-15). Interestingly, among the two latter forms protonated ions were more abundant for
203 short-chain Dols while potassiated ions – for long-chain ones (Fig. 3). Importantly, the
204 isotopic profiles of all the types of adducts (i.e., their isotopic envelopes) reflected that
205 observed for sodiated ions (Fig. 2 and Fig. 3). The observed complexity of the MS spectra
206 recorded in this report most probably mirrored the technical conditions of the analysis –
207 application of an instrument with particular parameters of the ion source and a high-
208 sensitivity detector.
209 In the MS spectra of metabolically labeled dolichols native Dols, with natural ^{13}C enrichment
210 (~1%) were found in addition to the [^{13}C]Dols formed due to utilization of [^{13}C]glucose (Fig.
211 2 and Fig. 3). They originated from the inoculum of the Arabidopsis hairy roots used to
212 initiate the culture growth (Skorupinska-Tudek et al., 2008).
213 The same ratio of signal intensities of sodiated $[M+Na]^+$ vs. ammoniated $[M+NH_4]^+$ ions was
214 found for a given Dol-n species across all n values (Fig. 4) suggesting the reproducibility of
215 the experimental conditions at the biological and analytical level.
216 Because of the co-occurrence of several types of Dol cationic adducts in the mass
217 spectrum the analysis of the isotopic envelope (the *m/z* value corresponding to its maximum)
218 used in our previous study (Skorupinska-Tudek et al., 2008) could not be applied. Therefore a
219 new method based on numerical simulation of the shape of the isotopic envelope, taking into
220 account all the cationic forms of the Dol ions, was used for further analysis.
221
222 *Labeling with [U-$^{13}C_6$]glucose*

223 Mass spectra of [^{13}C]Dols obtained from roots grown on [U-$^{13}C_6$]glucose as the sole
224 carbon source comprised a complex set of signals (Fig. 3, for explanation refer to Fig. 2). As
225 expected, signals corresponding to the maximal *m/z* predicted for uniformly labeled [U-
226 $^{13}C_{5n}$]Dol-n were identified, but numerous isotopic signals of "hypo-labeled" [^{13}C]dolichol
227 isotopomers were observed as well (Fig. 3). To investigate this phenomenon further
228 theoretical spectra of [^{13}C]Dols (i.e., theoretical isotopomer distributions) were calculated
229 (Methods, equations 1 and 2).

230 In control conditions (roots grown in the medium devoid of sorbitol) for each Dol-n
231 the maximum of the isotopic envelope of the experimental spectrum for the $[M+Na]^+$ and
232 $[M+NH_4]^+$ ions was located at a *m/z* lower than that calculated for the 99% [^{13}C] isotopic
233 abundance of the precursor [U-$^{13}C_6$]glucose (Fig. 5A for Dol-15). We therefore re-calculated
234 the spectra but with the assumption that the probability of ^{13}C incorporation in any given
235 position of Dol-n was identical but lower than the declared 99% value (see Methods)
236 corresponding to the isotopic abundance of the precursor glucose. This assumption took into
237 account possible dilution of the exogenous [^{13}C]substrate with endogenous glucose (with
238 natural isotopic ^{13}C abundance ~1%). These theoretical spectra were optimized to achieve the
239 best agreement with experimental ones (see Fig. 5B for Dol-15 and Supplementary Fig. 3 for
240 Dol-n) and the best fit was obtained for the [^{13}C] enrichment of 93.9 ± 1.0% for all Dol-n.
241 This value of the effective [^{13}C] abundance was used further. The maxima of the isotopic
242 envelopes of the theoretical mass spectra of Dol-n were in good agreement with the
243 experimental ones, but were slightly narrower than the latter as shown for Dol-15 in Fig. 5B
244 (even more obvious for stress conditions, Fig. 5E). This discrepancy suggested that besides
245 native glucose other native precursors, e.g. acetyl-CoA, trioses or IPP, were incorporated into
246 Dol (see Fig. 5C).

In the presence of 0.3 M sorbitol a striking shift of the mass spectrum of [^{13}C]Dol towards lower *m/z* values comparing to control conditions was observed (for Dol-15, compare Fig. 5D and 5A). This shift was similar for all analyzed Dol-n (Fig. 3) suggesting a further dilution of the [^{13}C]substrate/intermediate pool with their unlabeled counterparts upon sorbitol treatment. Theoretical spectra (Fig. 5E for [^{13}C]Dol-15 and Supplementary Fig. 3 for all Dol-n) calculated as above to fit the experimental ones revealed the effective [^{13}C] enrichment of 80.7 ± 1.3%.

The differences between the mass spectra of [^{13}C]Dols from sorbitol-treated vs. control tissues (Fig. 3) were statistically significant for each Dol-n ($\alpha < 10^{-5}$) according to the Mann-Whitney test applied for pairs of corresponding cumulative distributions (Fig. 6). Importantly, similar values of the effective ^{13}C isotopic abundance, 94.5 ± 1.3% and 79.0 ± 1.2% for the control and sorbitol-treated roots, respectively, were found for phytosterols synthesized in the presence of [U-$^{13}C_6$]glucose, confirming the universal nature of the observed metabolic effects of sorbitol (Fig. 8).

In summary, the [U-$^{13}C_6$]glucose experiments led to the conclusion that sorbitol treatment decreases the ^{13}C enrichment of [^{13}C]Dol from 93.9 ± 1.0% to 80.7 ± 1.3% most likely due to the mobilization of internal carbon sources, most probably through starch hydrolysis upon osmotic stress (Krasensky and Jonak, 2012). Sorbitol itself is unlikely to serve as a carbon source since its uptake from the medium is low and further decreased in the presence of glucose (Maurel et al., 2004). With the methodology applied here the Dol labeling derived from [U-$^{13}C_6$]glucose is biosynthetic route-insensitive (MEP vs. MVA), in contrast to NMR-based approach (Bacher et al., 2016), but enables quantitative analysis of the cellular effects of sorbitol. To elucidate the contribution of the MEP and MVA pathways to Dol biosynthesis [1-^{13}C]glucose-labeling followed by MS analysis was employed.

Labeling with [1-^{13}C]glucose

^{13}C atoms from [1-^{13}C]glucose were incorporated into all analyzed Dols (Dol-13 to Dol-23, Fig. 3). Theoretical mass spectra of Dol-15 and Dol-20 synthesized from [1-^{13}C]glucose exclusively via either the MEP ('lighter' isoprene units with two carbon atoms labeled, Fig. 7A and 7A', respectively) or the MVA ('heavier' units with three carbon atoms labeled, Fig. 7B and 7B') pathway were calculated (Methods, equations 1 and 2) using the effective ^{13}C abundances estimated (expected labeling pattern is shown in Fig. 1B). For dominating Dols (shown for Dol-15, Fig. 7A and B) upon control conditions the experimentally recorded spectrum was located between the two theoretical mass spectra calculated for Dol synthesized via either the MEP or MVA pathway (Fig. 7C) while upon stress experimental spectrum was matching exactly the theoretical one modelled for Dol synthesized exclusively via the MEP pathway (Fig. 7D). However, for longer Dols, upon both incubation conditions, control (shown for Dol-20, Fig. 7A' and B') and osmotic stress (Fig. 7D' and 7E'), the recorded spectra located between the two theoretical distributions (Fig. 7C', 7F') and indicated, in accordance with our earlier results (Skorupinska-Tudek et al., 2008), a mixed biosynthetic origin of Dol. The same was observed for all other [^{13}C]Dol-n (data not shown). Notably, in the presence of sorbitol the experimental mass spectra of [^{13}C]Dol were shifted towards lower *m/z* than these of the control (medium devoid of sorbitol, Fig. 3), similarly to the results for labeling with [U-$^{13}C_6$]glucose. This effect cannot by attributed to sorbitol-induced isotopic dilution or loss of ^{13}C atoms due to glucose catabolism via the oxidative pentose pathway since these effects were already been taken into account, by adjusting the effective ^{13}C isotopic abundance to 80.7%. However, contribution of native IPP would result in an additional decrease of the ^{13}C enrichment of Dol without, however, a broadening of the MS envelope that was observed for [U-$^{13}C_6$]glucose labeling.

297 *Co-operation of the MEP and MVA pathways to synthesize Dol*

298 To quantitate the MEP and MVA input to Dol formation theoretical isotopomer
299 distributions showing reasonable agreement with the experimental ones were calculated for
300 all Dols following equation (3) in Methods (Fig. 7C and 7F for Dol-15; Fig. 7C' and 7F' for
301 Dol-20; Supplementary Fig. 3 for all Dols).

302 For control conditions the number of isoprene units derived from the MEP pathway
303 giving the best fit to the experimental spectra, n_{MEP}, is 11 or 12 for most of the Dol-n species.
304 Consequently, the number of units derived from the MVA pathway, n_{MVA}, increases with the
305 length of dolichol from 3 (Dol-14) to 15 (Dol-23) (Table 2). This supports our put forward
306 earlier (Skorupinska-Tudek et al., 2008) hypothesis, that regardless of the length of Dol, the
307 MEP pathway mediates the synthesis of a common intermediate, while the number of MVA-
308 derived units is variable. It is therefore the cytoplasmic MVA-derived IPP and cytoplasmic
309 *cis*-prenyltransferase(s) (CPTs) that are responsible for the observed breadth of the Dol family
310 homologs. Interestingly, the contribution of the MEP pathway seems considerably higher for
311 *A. thaliana* (11-12 i.u.) than that for *C. geoides* (6-8 i.u.) roots (Skorupinska-Tudek et al.,
312 2008), although overall the biosynthesis of Dol seems to be performed in a similar manner in
313 this two plant species. The shortest species Dol-13, seems to an exception since it contained
314 only ~9 MEP-derived units and this number was not increased upon stress (see further).

315 In the presence of sorbitol the calculated n_{MEP} was 13-15 for Dol-14 - 17 (the
316 dominating dolichols) suggesting a substantially increased contribution of the MEP pathway
317 to their biosynthesis. In contrast, no such increase was observed for the longer Dols, Dol-18 –
318 23 (Table 2).

319 In accordance with the glycolytic catabolism of glucose with a stochastic mixing of triose
320 pools, the ^{13}C enrichment of Dols synthesized from [1-^{13}C]glucose was close to one half of

the calculated effective ^{13}C abundance both in the control (47.1 ± 0.9% vs. 93.9 ± 1.0%) and stress (40.2 ± 0.8% vs. 80.7 ± 1.3%) conditions (Fig. 5C and 5F, respectively).

Taken together these data indicate modulation of the relative activity of the isoprenoid-generating pathways in plant roots in response to osmotic stress resulting in an increased contribution of the MEP pathway to the biosynthesis of dominating Dol achieving virtually 100% for Dol-14 and -15. Strikingly, the metabolic origins of both short (Dol-13) and long-chain Dols (Dol-18 – 21) remain unaffected by sorbitol (Supplementary Fig. 4).

Sorbitol treatment also increased the contribution of the MEP pathway to phytosterol biosynthesis, but in this case only qualitative analysis was possible (see further).

Application of pathway-specific precursors

In order to elucidate further the effect of osmotic stress on the contribution of the two pathways to Dol biosynthesis Arabidopsis roots were grown in medium supplemented with deuterated precursors specific to either the MEP (deoxyxylulose, [$^2H_2$]DX) or the MVA pathway (mevalonolactone, [^{2}H]MVL) in the absence or presence of 0.3 M sorbitol. Deuterated dolichols were isolated and analyzed by MS. Consistently with the results of labeling with general precursor glucose the presence of various cationic derivatives (the NH_4^+, Na^+ and K^+ as well as traces of H^+ ones) resulted in a subtle structure of the spectra (Fig. 3). It should be kept in mind that the Dol molecules also contained ^{13}C atoms due to the natural abundance of ^{13}C (Fig. 2).

Labeling with [$^2H_2$]DX: the presence of signals of a higher *m/z* in the mass spectra, additionally to those corresponding to native Dol molecules, clearly confirmed precursor incorporation (Fig. 3, two deuterium atoms per isoprene unit are expected). Efficient labeling both in control conditions and stress was observed for Dol-15 – 17 (Fig. 2 for Dol-15), since

346 only for those Dols signals corresponding to fully labeled molecules were observed at *m/z* =
347 M + 2n, where M is the *m/z* of sodiated monoisotopic [^{12}C]Dol-n, and the relative content of
348 the fully labeled Dol-15 - 17 in the total Dol mixture was substantially increased in stress
349 conditions (Fig. 3). Dol-18 was efficiently labeled only upon osmotic stress, while the longer
350 Dols were not labeled from this precursor.

351 The observed increased deuterium incorporation to Dol-15 – 17 upon osmotic stress
352 supports the increased contribution of the MEP pathway to their biosynthesis, confirming the
353 results obtained by [1-^{13}C]glucose feeding. On the other hand, the divergent labeling of
354 various Dol species again suggests that individual Dol families are synthesized by different
355 CPTs, which are independently regulated and have different access to the DX precursor,
356 possibly due to their sub-compartmentalization.

357

358 **Labeling with [^{2}H]MVL:** the labeling pattern was different from that observed for
359 DX labeling (Fig. 2 and Fig. 3, one deuterium atom per isoprene unit is expected). Fully
360 labeled Dol-15 – Dol-18 molecules (*m/z* = M + n) were synthesized both in the control and
361 osmotic stress conditions, and [^{2}H]Dol-14 was observed in the control conditions only. This
362 observation suggested that under these feeding conditions (i.e., in the presence of the
363 exogenous MVL) Dol-15 – Dol-18 originate mostly from the MVA pathway. Interestingly,
364 Dols longer than Dol-18 were only partially labeled and both the extent of the labeling and the
365 fraction of the labeled molecules decreased with increasing n (Fig. 3). Osmotic stress
366 exacerbated this relation supporting the decreased contribution of the MVA pathway in Dol
367 biosynthesis in these conditions. Moreover, similarly as observed above, osmotic stress
368 induced the synthesis of the dominating Dols (Dol-15 -17) only.

369 As shown above, signals corresponding to maximally deuterated Dol-15 – Dol-17
370 molecules (in accordance with the labeling pattern expected for the applied precursor) were

371 recorded for both precursors in control conditions and stress. It should be noted, however, that
372 feeding specific precursors can alter the regulation of the isoprenoid-generating pathways and
373 in these conditions their relative contribution need not reflect the native situation (Lipko &
374 Swiezewska, 2016). Consequently, quantitative elucidations aimed at estimation of the
375 number of MEP- vs. MVA-derived isoprene units could not be performed using pathway-
376 specific precursors.
377
378 ***Effect of sorbitol on the biosynthesis of phytosterols***
379 In order to elucidate whether sorbitol affected the global isoprenoid metabolism, its
380 effect on the biosynthesis of phytoterols (β-sitosterol, stigmasterol and campesterol) was
381 analyzed using GC/MS in addition to the study of Dols. It should be noted that the level of
382 ^{13}C labeling of stigmasterol was substantially lower than that of the two remaining sterols.
383 Sorbitol treatment shifted the isotopic envelopes for all analyzed [^{13}C]phytosterols labeled
384 with [U-$^{13}C_6$]glucose (Fig. 8A). Estimation of the ^{13}C isotopic enrichment of phytosterols,
385 reflecting the effective ^{13}C isotopic abundance of their biosynthetic precursor was performed
386 similarly as for Dols and revealed 94.5 ± 1.3% and 79.0 ± 1.2% for the control and sorbitol-
387 treated roots, respectively. Importantly, similar values of the effective ^{13}C isotopic abundance
388 of glucose 93.9±1.0% vs. 80.7 ± 1.3% were found based on the isotopic enrichment of
389 [^{13}C]Dol labeled with [U-$^{13}C_6$]glucose, confirming the universal nature of the observed
390 metabolic effects of sorbitol.
391 The values of the effective ^{13}C abundance estimated above were further used to
392 calculate the theoretical mass spectra of [^{13}C]phytosterols synthesized from [1-^{13}C]glucose as
393 the precursor. Similarly as for Dol, the theoretical spectra were calculated for all three
394 phytosterols assuming their exclusive origin from either the MVA or MEP pathway.

In control conditions the maximum of the experimental mass spectrum was located between the theoretical envelopes calculated for the MVA and MEP pathways for each phytosterol (Fig. 8A, second left column). This suggested that in fact IPP derived from the both pathways contributed to phytosterol biosynthesis in the applied experimental model.

Upon sorbitol treatment the experimental isotopic envelope was shifted to lower *m/z* values for all phytosterols analyzed, suggesting an increased contribution of the MEP pathway to phytosterol biosynthesis under osmotic stress since, similarly to Dols, the observed shift cannot be explained solely by the apparent decrease of ^{13}C abundance.

A note of caution is due here that the quantitative modeling of the relative contribution of the MEP and MVA pathways to phytosterol biosynthesis using the methodology applied in this report to Dol is of poor reliability. The main reason for this is the fact that only 10 or 15 carbon atoms per molecule of phytosterol can be labeled from [1-^{13}C]glucose *via* the MEP or the MVA pathway, respectively. Assuming that the ^{13}C enrichment follows binomial distribution with 10 (MEP) and 15 (MVA) tries with p=0.5, a difference of 2.5 Da is obtained between the maxima of the calculated spectra for the two pathways while the expected half-width of the isotopic envelopes is 4 and 5 Da, respectively, for the MVA and MEP pathways (Fig. 8B).

Consequently, such a small difference makes impossible a quantitative estimation of the relative contribution of the two pathways.

To elucidate the effect of pathway-specific precursors on phytosterol biosynthesis GC/MS analysis of sterols isolated from roots fed [$^2H_2$]DX or [^2H]MVL was performed (Fig. 8A). Interestingly, the level of deuterium labeling of stigmasterol was lower than that of campesterol while the labeling of sitosterol was considerably higher. Sorbitol treatment resulted in a modest decrease of deuterium incorporation from [^2H]MVL (approx. 85-90 % of

419 control for all sterols) while that from [$^{2}H_{2}$]DX was slightly enhanced (approx. 130% and
420 115% of control for stigmasterol and β-sitosterol) (Fig. 8A).
421 Moreover, while the total content of phytosterols was not affected by sorbitol (Table 1) the
422 labeling rate (*de novo* biosynthesis) of sitosterol was considerably enhanced in contrast to
423 decreased labeling of stigmasterol (Fig. 8A). In line with this the proportion among the
424 phytosterols changed. In control conditions stigmasterol was the dominant species (43.1% of
425 total phytosterol content) while in sorbitol-treated roots β-sitosterol dominated (49.5% of
426 total).

427 Taken together, analysis of metabolically labeled phytosterols suggests that in the
428 biological system studied both the MVA and MEP pathways contribute to their biosynthesis.
429 Although phytosterols are usually considered to be exclusively MVA-derived, an equal
430 contribution of the MVA and MEP pathways to their biosynthesis has already been reported
431 in Croton callus culture (De-Eknamkul and Potduang, 2003). While the relative contribution
432 of the MEP and MVA pathways to phytosterol biosynthesis could not be quantitated it was
433 clear that osmotic stress enhanced the MEP pathway input.
434

435 **Discussion**

436 In this report the co-operation of the MEP and MVA pathways was gauged using
437 dolichol as a reporter molecule. The key finding is that increased contribution of the MEP
438 pathway, at the expense of MVA, to Dol biosynthesis observed upon osmotic stress was
439 estimated quantitatively. Moreover, since the biosynthesis of solely one family of Dols (Dol-
440 14 – 17) was affected without modulation of the biosynthetic route of either short- (Dol-13) or
441 long-chain (n> 17) Dols it further validates the applied method.
442 To allow the quantification of MEP- and MVA-derived isoprene units a novel method
443 involving numerical modeling of mass spectra of [^{13}C]Dols metabolically labeled with

444 [^{13}C]glucose was established. Basing on the biochemistry of the isoprenoid biosynthesis and
445 using simple statistics tools theoretical mass spectra (iterative models) of the labeled dolichols
446 were calculated and fitted to the experimentally recorded ones. The two-step protocol
447 involved application of [U-$^{13}C_6$]glucose to estimate the effective ^{13}C abundance and then of
448 [1-^{13}C]glucose to analyze quantitatively the input of the two different routes of IPP synthesis.
449 The first step was essential since sorbitol affected the cellular metabolism, most probably by
450 increasing the release of glucose from native starch (Krasensky and Jonak, 2012; Valentovic
451 et al., 2006) present in the root inoculum. Besides, sorbitol might also stimulate the activity of
452 the other, apart from glycolysis, catabolic processes utilizing glucose, e.g. oxidative pentose
453 pathway and this in turn will result in shuffling of carbon atoms in glucose molecules. Indeed,
454 abiotic stress was shown to induce the expression of the oxidative pentose phosphate genes
455 (Caretto et al., 2015). The resulting isotopic dilution of the labeled precursor would affect the
456 subsequent calculations – had it not been corrected for. It should also be underlined that
457 externally applied sorbitol does not serve as a carbon source for root metabolism since its
458 uptake from the medium is low and is even further decreased in the presence of external
459 glucose (Maurel et al., 2004).

460 The results presented here suggest that a divergent biosynthetic machinery is engaged
461 in the formation of Dol families of different lengths. Consequently, the MEP and MVA-
462 derived pools of IPP could be used by dedicated CPTs. The changing Dol composition and
463 labeling profiles suggest an involvement of at least three such enzymes in Arabidopsis roots,
464 similarly to the two yeast CPTs, Rer2 and Srt1, responsible for the formation of two Dol
465 families in *S. cerevisiae* (Schenk et al., 2001). Furthermore, the observed specific changes of
466 CPTs' transcript levels in response to osmotic stress could underlie the adjustment of the Dol
467 spectrum to current requirements. This is most probably achieved by CPT
468 compartmentalization (Fig. 9), although several aspects of this model remain elusive (e,g.,

peroxisomal CPT and PPRD, IPP and oligoprenylPP transporters). Besides plastids and ER, postulated earlier to harbor CPTs (Skorupinska-Tudek et al., 2008), also plant peroxisomes could possess their own CPT, as was observed in mammals and yeast (Ericsson et al., 1992; Skoneczny et al., 2006). Moreover, the existence of the peroxisomal pathway converting mevalonate to IPP in mammals and plants (Thompson et al., 1987; Simkin et al., 2011) further supports this concept. Still the type of the all-*trans* initiator involved in biosynthesis of Dols in Arabidopsis roots remains enigmatic.

Deduced topological model of Dol biosynthesis (Fig. 9) presents a simplified scenario presuming that the homogenous polyisoprenoid chain built of IPPs of solely MEP-origin is formed in the plastid. Actually, one cannot exclude the possibility that, especially upon stress, longer polyisoprenoid chains, comprising 11-12 MEP-derived isoprene units together with a few isoprene units of the MVA origin are formed in this compartment.

The multifamily composition of Dol mixture together with different sites of their biosynthesis could also implicate different cellular roles of Dols of various length. The dominating homologues, Dol-14 -17, most probably act as cofactors in protein glycosylation in the ER, as is observed in yeast (Schenk et al., 2001). *N*-glycans are crucial for plant growth under stress conditions (Strasser, 2016) and therefore reprogramming of the Dol-14 -17 biosynthetic route could be indispensable for plant homeostasis. Long- and short-chain Dols are most possibly not involved in protein glycosylation (Schenk et al., 2001; Surmacz et al., 2014) but instead could act as a shield against ROS or fulfill other as yet unknown functions.

The concomitant modulation of the activity of MVA and MEP pathway is a subject of extensive studies - the rate of precursor exchange may reach 100% and 80% from the plastids to the cytoplasm and *vice versa* (Schuhr et al., 2003; Hemmerlin and Bach, 2000), although these values were observed upon inhibitor treatments. Various intermediates, e.g., IPP, DMAPP, GPP, FPP, oligoprenyl diphosphates (Hemmerlin et al., 2012; May et al., 2013)

were shown to be translocated between these compartments. Moreover, a complex bidirectional transfer of precursors has been postulated earlier (Skorupinska-Tudek et al., 2008) as well as in the current model (Fig. 9). The observed increased contribution of the MEP pathway towards Dol biosynthesis upon sorbitol treatment corroborates earlier data suggesting transcriptional stimulation of the MEP pathway by osmotic stress (Wu et al., 2009; Yan et al., 2009) and heavy metals (Ge and Wu, 2005) leading to accumulation of tanshinone, a diterpenoid, in *Salvia miltiorrhiza* hairy roots**.** Likewise, osmotic stress, heavy metal salts and ABA treatment increased the accumulation of brachycerine, a monoterpene indole alkaloid, in the leaves of *Psychotria brachyceras* (do Nascimento et al., 2013). Similarly, increased expression of the MEP pathway and carotenoid biogenesis genes was noted in osmotically stressed Arabidopsis roots (Meier et al., 2011). In contrast, the literature data on the effect of osmotic stress on the MVA pathway seem contradictory. Thus, in line with the decreased contribution of the MVA pathway to the biosynthesis of the dominating Dols reported here, down-regulation of *Brassica juncea* 3-hydroxy-3-methylglutaryl coenzyme A synthase (the key regulator of the MVA pathway) was observed (Alex et al., 2000; Nagegowda et al., 2005). Conversely, water stress (mimicked by PEG treatment) induced both the MVA and the MEP pathway and led to an increased accumulation of tanshinone, although MEP seemed to be the main contributor (Yang et al., 2012).

Various mechanisms could underlie the stimulation of the MEP pathway at the expense of MVA upon osmotic stress. First, it could be linked to the cellular 'energy-saving' program since an enhanced need for ATP is to be expected upon stress and formation of IPP via the MEP pathway requires less ATP than *via* the MVA pathway (2 vs. 3 moles per mole of IPP) (Gruchattka et al., 2013). Second, it could result from activation of a 'sink-like' rescue pathway involving enhanced synthesis of reduced compounds, such as isoprenoids, in order to consume $NADPH^+$ overproduced upon stress (Selmar and Kleinwaechter, 2013).

519 Consumption of reducing equivalents by the MEP pathway is more efficient than by MVA (3
520 vs. 2 moles of NADPH are used to produce one mole of IPP, respectively) (Gruchattka et al.,
521 2013). Finally, an enhanced demand for MEP-derived products such as the antioxidants
522 tocopherols and carotenoids and/or phytohormone abscisic acid could also provide the driving
523 force for the induction of this pathway (Abbasi et al., 2007).

524 The signaling route(s) responsible for the regulation of the MEP/MVA balance
525 remains elusive, albeit phytohormones should be considered as putative regulators. Abscisic
526 acid (ABA, synthesized via the MEP pathway), has been found to induce the biosynthesis of
527 MEP-derived metabolites, and both ABA-dependent and -independent signaling pathways
528 appear to be involved in osmotic stress tolerance (Huang et al., 2012). Gibberellic acid has
529 been reported to inhibit the biosynthesis of MEP-derived isoprenoids and to stimulate the
530 MVA pathway (Mansouri et al., 2009). Additionally, ROS could also play a role of such
531 regulators since their signaling network controls diverse stress responses (Lin and Aarts,
532 2012). One is also tempted to speculate that methylerythritol cyclodiphosphate (MEcPP), a
533 product of the MEP pathway so far recognized as a retrograde-signaling metabolite inducing
534 expression of selected abiotic stress-responsive genes (Xiao et al., 2012), could be involved.
535 Notably, MEcPP potentiates the unfolded protein response (Walley et al., 2015) induced upon
536 osmotic stress in plants (Moreno and Orellana, 2011) and, interestingly, Dol attenuates this
537 stress reaction (Jozwiak et al., 2015).

538 In conclusion, Dol is the compound of choice to analyze quantitatively the co-
539 operation of the MEP and MVA pathways owing to its mixed MEP/MVA origin and the large
540 number of carbon atoms per molecule allowing the use of reliable iterative models (e.g., for
541 Dol-16 the number of carbon atoms labeled by [1-^{13}C]glucose equals 32 or 48 for the MEP or
542 the MVA pathway, respectively). Furthermore, the occurrence of a complex mixture of Dols
543 in plant tissues (thirteen homologues in Arabidopsis roots) enables cross-validation of the

obtained models. Since dolichols are common component of plant roots application of the experimental approach described here, i.e., metabolic labeling followed by meta-analysis of Dol mass spectra, seems feasible for other plant species. It should be kept in mind, however, that modulation of the contribution of the MEP and MVA pathway, recorded for Dol biosynthesis, should be critically interpreted. Although Dol might be considered as an indicator sensing the reprograming of the isoprenoid generating systems in plants the input of the MEP-derived precursors, despite the overall increase, might differ quantitatively for particular subclasses of isoprenoids (in fact observed for different Dol 'families'); this difference might result from divergent subcellular localization of these compounds.

Moreover, methodology described in this report is based on the metabolic labelling with glucose. Such approach is clearly applicable to heterotrophically grown tissues/cells while feeding of intact plants or detached photosynthetic organs might be more complex due to several reasons. Firstly, the uptake of glucose by intact plant might be low since plants generate their biomass exclusively from CO_2. However, metabolism of [^{13}C]glucose observed in the leaves of aseptically grown intact tobacco plants fed [U-$^{13}C_6$]glucose via the root system provided a proof of concept for this labeling method (Ettenhuber et al., 2005), and applicability of this approach was confirmed later too (summarized in Bacher et al., 2016). Incorporation of [^{13}C]glucose upon these circumstances might possibly be explained by different biosynthetic origin of the MEP pathway substrates - glyceraldehyde 3-phosphate (GAP) is derived mostly from photosynthesis while pyruvate originates from glycolysis (Pokhilko et al., 2015).

Secondly, incorporation of [^{13}C]glucose together with the concomitant influx of the unlabeled precursors derived from photosynthesis/glucogenesis would result in the substantially lower ^{13}C enrichment of Dols or Prens. Consequently, a small *m/z* difference between the maxima of the theoretical envelopes calculated for the MEP- and MVA-derived Dol molecule might be

569 expected (e.g., 1 Da for Dol-20 labeled from [1-^{13}C]glucose of 10% isotopic ^{13}C abundance,
570 Supplementary Fig. 5, left panels). Therefore distinction of these pathways would not be
571 reliable. Fortunately, this problem might be partially overcome by feeding with doubly
572 labeled precursor (e.g., [1,6-$^{13}C_2$]glucose, Supplementary Fig. 5, right panels) – in such case
573 the expected *m/z* difference is larger (e.g., 2-3 Da) and enables qualitative/semi-quantitative
574 depiction of the biosynthetic origin of Dol. Additionally, such analysis would be much easier
575 presuming that the spectrum comprises signals of a single cationic form of Dols (likely after
576 technical modifications of the HPLC/MS analysis).

577 Secondary metabolites, including polyisoprenoids, play important roles in the
578 adaptation of plants to diverse environmental stimuli and in overcoming stress conditions.
579 Numerous studies have been undertaken to dissect the plant metabolic responses to abiotic
580 stresses, which involve intra- and extracellular signaling, and modification of the cell
581 metabolism (Obata and Fernie, 2012), including the modulation of the activity of MEP and
582 MVA pathways.

583 This report describes a new approach to studying the co-operation of the MEP and MVA
584 pathways and adds new players – dolichols – to the complex network of the plant response to
585 osmotic stress.

586

587 **Methods**

588 **Plant material and growth conditions**

589 *In vitro* culture of *Arabidopsis thaliana* hairy roots was propagated as described
590 previously (Jozwiak et al., 2013). For metabolic labeling with a general precursor roots were
591 grown in ½ Murashige-Skoog (MS) medium supplemented with either 2% [1-^{13}C]glucose or
592 2% [U-$^{13}C_6$]glucose used as a sole carbon source. For labeling with pathway-specific
593 precursors ½ MS medium was supplemented with 2% glucose (natural ^{13}C abundance) and

one of the precursors, either [5-^{2}H]mevalonate (final concentration 1 mM) or [5,5-$^{2}H_2$]deoxyxylulose (final concentration 0.5 mM). Labeling was performed for two weeks (at this time point glucose concentration was 1.7%) in parallel in the above-described media (control) or in the same media supplemented with 300 mM sorbitol. At this sorbitol concentration Dol accumulation was increased without unfavorable effects on the growth of the hairy root culture.

To elucidate the effect of other stressor on Dol metabolism ½ MS medium containing 2% glucose (natural ^{13}C abundance) was supplemented for two weeks with various chemicals at indicated final concentrations: cadmium chloride (25 or 50 μM) or oxidative agents – hydrogen peroxide (1 mM), *tert*-butyl hydroperoxide (tBHP, 0.3 mM) or methyl viologen (MV, 1 μM).

Chemicals

All dolichol and polyprenol standards were from the Collection of Polyprenols (Institute of Biochemistry and Biophysics, Polish Academy of Sciences, Warsaw). Standards of phytosterols were from Sigma-Aldrich. D-[1-^{13}C] and D-[U-$^{13}C_6$]glucose were from Cambridge Isotope Laboratories (Retaveni, Warsaw, Poland). [5-^{2}H]mevalonate and [5,5-$^{2}H_2$]deoxyxylulose were synthesized using the protocols published earlier (Keller, 1986; Meyer et al., 2004) with modification: NaB[$^{2}H]_4$ instead of NaB[$^{3}H]_4$ was used as a substrate to prepare labeled mevalonate. TLC plates (silica gel and RP-18) and gels for column chromatography (silica gel 60 and Florisil) were from Merck (Warsaw, Poland), organic solvents (HPLC and p.a. grade) were from POCh (Gliwice, Poland). Murashige-Skoog Basal Salt Mixture and all other chemicals were purchased from Sigma-Aldrich (Poznan, Poland) and were of analytical grade.

Isolation and purification of native and metabolically labeled dolichols and phytosterols

618 Roots were harvested, rinsed with water, dried with a paper towel, weighed and
619 homogenized. Dolichols and phytosterols were isolated as described earlier (Jozwiak et al.,
620 2013) with modifications. Briefly, to isolate Dols unsaponifiable lipids were purified on a
621 silica gel column eluted with hexane containing increasing concentrations of diethyl ether (0–
622 25%). Fractions containing dolichols (according to TLC on silica gel plate developed in
623 toluene:ethyl acetate, 9/1, v/v and stained in iodine vapors) were combined, evaporated under
624 a stream of nitrogen, dissolved in propan-2-ol and subjected to HPLC/UV purification.
625 Internal standards (Prenol-19, 10 μg or cholestanol, 10 μg) were added prior to
626 homogenization only when the content of Dol or phytosterols was to be estimated. Polyprenol
627 (Pren-9, 11-23, 25) and dolichol (Dol-15 to Dol-24) mixtures were used as external standards.

628 **HPLC/ESI-MS analysis of [^{13}C]- and [^{2}H]dolichols**

629 LC/MS analysis of polyisoprenoids was performed on an Ultra-Performance Liquid
630 Chromatograph ACQUITY UPLC I-Class (Waters Inc.) coupled with a MALDISynapt G2-S
631 HDMS (Waters Inc.) mass spectrometer equipped with an electrospray ion source (ESI) and
632 q-TOF type mass analyzer. The separation of polyisoprenoid alcohols was carried out using a
633 100 mm x 2.1 mm BEH C18 column (Waters Inc.). Solvent A was a methanol and water
634 mixture (9/1, v/v) and solvent B – methanol/isopropanol/hexane (2/1/1, v/v/v) combined as
635 follows: from 0% B to 75% B in 10 min, from 75% B to 90% B in 5 min, from 90% B to
636 100% B in 1 min and 100% B maintained for 4 min, then from 100% B to 0% B in 1 min. The
637 polyisoprenoids were injected in a mixture of methanol/chloroform (1/1, v/v). The LC/MS
638 analysis was carried out at a flow rate of 0.4 ml/min.
639 Mass spectra of polyisoprenoid alcohols were recorded in the positive ion mode. The
640 desolvation and cone gas was nitrogen. The measurements were performed at the desolvation
641 gas flow of 448 L/h, the cone gas of 76 L/h and the nebuliser gas pressure of 4.6 bar. The
642 capillary voltage was set to 3800 V and the sampling cone at 87 V.

643 The instrument was controlled and recorded data were processed using the MassLynx V4.1
644 software package (Waters Inc.).

645 **GS-FID/MS analysis of [^{13}C]- and [^{2}H]phytosterols**

646 The GC-MS analysis was carried out on an Agilent 7890A gas chromatograph coupled
647 to an Agilent 5975C MS detector under electron impact ionization (70 eV). The MS scan
648 range was 33-500 atomic mass units. The chromatographic column was a HP-5MS UI
649 capillary column (30 m, 0.25 mm, 0.25 μm). The carrier gas was helium at a flow rate of 1.0
650 ml/min. FID gases flow rate was maintained at 30 and 400 ml/min for hydrogen and air,
651 respectively. Samples were analyzed with the column held at 265°C for 60 minutes. The
652 injection was performed in the split mode (10:1) at 290°C. The inlet temperature was set at
653 250° while that of the MS transfer line, quadrupole and ion source was 275, 150 and 230°C,
654 respectively. The identification of the compounds was achieved by comparison of their mass
655 spectra with the NIST 2008 Library (version 2010, Wiley 9th ed.) as well as by comparison of
656 retention times with commercially available standards.

657 **GC-FID analysis of sugars in culture medium**

658 Aliquots of culture medium (25 μl) containing glucose and internal standard (25 μl of
659 2% xylose) were placed in a glass vial. Water was evaporated under a stream of nitrogen and
660 the vial was placed in desiccator at 30 mbar. After 48 h pyridine (462 μl),
661 hexamethyldisilazane (92 μl) and chlorotrimethylsilane (46 μl) were added. Firmly closed vial
662 was heated for 30 minutes at 60°C in a heating block. Products of derivatization were
663 analyzed by GC-FID.

664 The GC apparatus was as in phytosterol analysis. Nitrogen was used as the carrier gas at an
665 average flow rate of 1.4 ml/min. Hydrogen and air flow-rate was maintained at 30 and 400
666 ml/min, respectively. The inlet and detector temperature was 210 and 290°C, respectively,
667 and the oven temperature was programmed at 150-210-275°C with a two-minute hold at

668 150°C, an increase rate of 6°C/min to 210°C and an increase rate of 40°C/min and a ten-
669 minute hold at 275°C.

670 **Analysis of MDA with thiobarbituric acid (TBA)**

671 Hairy roots (0.2 g fresh weight) were homogenized in 4 ml of 0.1% (w/v)
672 trichloroacetic acid (TCA) on ice. The homogenate was centrifuged at 10,000 x *g* for 5 min
673 and the supernatant was collected. One milliliter of 20% (w/v) TCA containing 0.5% (w/v)
674 TBA was added to a 0.5-ml aliquot of the supernatant. The mixture was kept in a boiling
675 water bath for 30 min and then quickly cooled on ice. After centrifugation at 10,000 x *g* for 10
676 min, the absorbance of the supernatant was measured at 532 and 600 nm. The absorbance at
677 600 nm was subtracted from the absorbance at 532 nm and the MDA concentration was
678 calculated using its extinction coefficient (155 mM^{-1} cm^{-1}) (Heath and Packer, 1968).

679 **Quantitative (qPCR) expression analysis of *cis*-prenyltransferases and polyprenol**
680 **reductase**

681 Total RNA was isolated and purified using the RNeasy Plant Mini Kit (Qiagen)
682 according to the manufacturer's instructions. RNA concentration and purity were verified
683 using a NanoDrop™ 1000 Spectrophotometer (Thermo Scientific, Waltham, MA). Before
684 cDNA synthesis, RNA was treated with RNase-free DNase I (Thermo Scientific) according to
685 the manufacturer's instructions and then the first-strand cDNA synthesis was carried out with
686 2 µg of RNA using the SuperScript™ III First-Strand Synthesis System for RT-PCR
687 (Invitrogen) and oligo-dT primers according to the manufacturer's procedure.
688 *CPTs* or *PPRD2* expression analysis was performed in a total volume of 20 µl of Luminaris
689 Color HiGreen high ROX qPCR Master Mix (Thermo Scientific) using gene-specific primers
690 (Jozwiak et al., 2013; Jozwiak et al., 2015) in a StepOnePlus Real-Time PCR System
691 (Applied Biosystems) according to the manufacturer's instructions.

692 The cycle threshold (Ct) was used to determine the relative expression level of a given gene
693 using the $2^{-\Delta\Delta Ct}$ method. The relative expression level of *CPTs* was analyzed after
694 normalization with *ACTIN-2* gene used as the internal reference. Statistical analysis of the
695 qPCR data was performed using one-way ANOVA with Tukey's post hoc test and GraphPad
696 Prism version 5.00 for Windows (GraphPad Software, San Diego, CA, www.graphpad.com).

697 **Numerical models**

698 The experimental mass spectrum of dolichol was modeled as the sum of theoretical
699 isotopomer distributions of each particular Dol-n, native and/or labeled, and in all cases
700 various cationic adducts (i.e., H^+, NH_4^+, Na^+, K^+) were considered.

701 For native (unlabeled) Dol-n its isotopomer distribution, B(*N*,*p*,*k*), was modeled according to
702 the binomial distribution with N trials and p≈1% (corresponding to natural ^{13}C abundance)
703 according to the equation (1):

704 $$B(N,p,k) = \binom{N}{k} \cdot p^k \cdot (1-p)^{(N-k)} \quad (1)$$

705 where *N*=5*n represents the number of carbon atoms in a Dol-n molecule and *k* is the number
706 of ^{13}C atoms incorporated.

707 Contribution of various cationic adducts was further taken into account as follows:

708 $$I(N,p,i) = I_H \cdot B(N,p,i) + I_{NH4} \cdot B(N,p,i-17) + I_{Na} \cdot B(N,p,i-22) + I_K \cdot$$

709 $$B(N,p,i-38) \quad (2)$$

710 where I_x stands for the relative amount of each cationic adduct and *i* represents the relative
711 increase of its mass in comparison to that of the protonated monoisotopic ^{12}C ion (*i*=0), and
712 *B*(*N*,*p*,*k*)=0 for *k*<0.

713 For labeled dolichols extracted from roots grown on [U-$^{13}C_6$]glucose the theoretical
714 isotopotomer distribution was obtained using the same model, but with *p*≈99%
715 (corresponding to the ^{13}C abundance of the precursor glucose declared by the producer).
716 Slight discrepancies in the level of labeling of individual carbon atoms in the precursor [U-

717 $^{13}C_6$]glucose could affect the final labeling probability but this was not taken into account in
718 the model.
719 For labeled dolichols extracted from roots grown on [1-^{13}C]glucose two classes of models
720 were considered to reflect the two possible routes of their generation: from IPP synthesized
721 exclusively via a single pathway (MEP or MVA) or, alternatively, from a mixed pool of IPP
722 derived through both these pathways. With [1-^{13}C]glucose as a precursor pathway-specific
723 labeling of IPP results in 2 or 3 ^{13}C atoms incorporated in a MEP- or MVA-derived isoprene
724 unit, respectively, assuming glycolysis as the only source of the intermediates for IPP
725 formation (Lipko and Swiezewska, 2016) (Fig. 1B).
726 In the 'pure' models for a Dol composed of n isoprene units (Dol-n) the number of sites
727 possibly enriched in ^{13}C atoms upon [1-^{13}C]glucose feeding (*N*) equals 2*n for the MEP
728 pathway and 3*n for the MVA pathway. In both cases the labeling probability is ½, reflecting
729 the metabolic equivalence of C-1 and C-6 atoms of glucose (Skorupinska-Tudek et al., 2008),
730 and the theoretical isotopomer distribution follows equations (1) and (2).
731 In the alternative model assuming a mixed origin of IPP forming a Dol-n molecule n_{MEP}
732 isoprene units originate from the MEP and n_{MVA} units from the MVA pathway, and $n = n_{MVA} +$
733 n_{MEP}. The theoretical isotopomer distribution can be thus expressed as a formal convolution of
734 two distributions corresponding to the two pathways according to the equation:
735 $$C(n_{MEP} + n_{MVA}, p, k) = \sum_{j=0}^{k}\{B(2 \cdot n_{MEP}, p, j) \cdot B(3 \cdot n_{MVA}, p, k-j)\} \quad (3)$$
736 with contribution of various cationic adducts calculated according to equation (2), keeping
737 $B(N,p,i) = 0$ for $i<0$. Please note, that for n_{MVA} or n_{MEP} equal 0, the equation (3) is equivalent
738 to equation (1).
739 **Modeling procedure**
740 Appropriate models were fitted to the set of experimental mass spectra using
741 Marquardt algorithm (Marquardt, 1963) implemented in the GnuPlot program [available at

742 http://gnuplot.info]. All Dol-n spectra were fitted simultaneously by optimization of I_x
743 contributions (equation 2, independently for each dolichol) and the common value for the ^{13}C
744 enrichment (*p* in equation 1 or 3), separately for each experimental condition. In the
745 convolution approach (equation 3), for each Dol-n all possible combinations of integer values
746 of n_{MEP} and n_{MVA} were tested to obtain the best fit (in terms of chi-square).
747

748 **Acknowledgements**

749 We would like to express our gratitude to Professor Michel Rohmer, Université de
750 Strasbourg/CNRS, Strasbourg and Professor Jolanta Maluszynska, University of Silesia,
751 Katowice, for stimulating discussions and collaboration. This investigation was supported by
752 grants from the National Science Centre of Poland [UMO-2012/07/B/NZ3/02437], [UMO-
753 2012/06/M/NZ3/00155] (ES) and [UMO-2011/03/B/NZ1/00568] (LS) and from the
754 Foundation for Polish Science grant [MPD/2009–3/2, project co-financed from the European
755 Union - Regional Development Fund] (AL).
756

757 **Author contributions**

758 A.J., T.C., J.P. and E.S. designed experiments; A.J. was responsible for tissue culture, feeding
759 experiments, lipid extraction and purification; A.J. and A.L. synthesized pathway-specific
760 precursors; T.C. contributed unique chemicals; M.K., W.D., J.W. and K.Z. performed
761 structural analysis of dolichols; C.P. performed GC-MS analysis of phytosterols; A.J., L.S.
762 and A.W. performed analysis of gene expression; A.J., A.L., J.P. and E.S. analyzed the data;
763 A.J., J.P. and E.S. wrote the manuscript.
764

765 **Competing financial interests**

766 The authors declare no competing financial interests.

767

768 **Additional information**

769 Supplementary information is available in the online version of the paper

770

771 **Figure legends**

772 **Figure 1**

773 **Polyisoprenoid alcohols of Arabidopsis hairy roots.** (A) Structure of prenols and dolichols
774 composed of n isoprene units. (B) Isoprene unit –carbon atoms potentially labeled upon
775 feeding [1-^{13}C]glucose are marked – note different labeling pattern *via* the MEP and MVA
776 pathways shown as vertical or horizontal striping, respectively. (C) Phylogenetic relationships
777 among the Arabidopsis and *S. cerevisiae cis*-prenyltransferases (Rer2 and Srt1) were
778 reconstructed using a multiple sequence alignment program, MAFFT (http://mafft.cbrc.jp/)
779 with L-INS-i alignment method. CPTs from *S. cerevisiae*: Rer2 and Srt1 (P35196 and
780 Q03175) and *A. thaliana*: AtCPT1, AtCPT2, AtCPT3, AtCPT6, AtCPT7 and AtCPT9
781 (O80458, F4IMI8, Q8S2T1, Q8RX73, Q56Y11and Q570Q8). Effect of sorbitol on: (D) Dol
782 accumulation, (E) relative expression of *cis*-prenyltransferases, *CPTs* (RT- qPCR) and (F) left
783 panel, relative content of dolichols and polyprenols (bars with white and gray background,
784 respectively) and right panel, relative expression of polyprenol reductase 2 *PPRD2* in hairy
785 roots under stress.

786 **Figure 2**

787 **Mass spectra of Dol-15 metabolically labeled from various precursors applied in the**
788 **absence (green trace - control) or presence of sorbitol (blue trace).**

789 A: native Dol-15, inset presents UV spectra of polyisoprenoid mixtures isolated from roots
790 gown in the absence or presence of sorbitol (green or blue trace, respectively). Signals

corresponding to the analyzed Dol families (dominating Dols and long-chain Dols) are indicated.

B: feeding [U-$^{13}C_6$]glucose

C: feeding [1-^{13}C]glucose

D: feeding [$^{2}H_2$]deoxyxylulose

E: feeding [^{2}H]mevalonolactone

M is the *m/z* of monoisotopic [$^{12}C_{75}$]Dol-15. Brackets above the spectra indicate signals of [^{13}C]Dol-15 isotopomers synthesized from precursors with natural [^{13}C] abundance.

(B) and (C) - arrows indicate signals corresponding to monoisotopic [$^{12}C_{75}$]- and [$^{13}C_{75}$]Dol-15 ions: protonated $[M+H]^+$ or $[M(^{13}C_{75})+H]^+$, ammoniated $[M+NH_4]^+$ or $[M(^{13}C_{75})+NH_4]^+$, sodiated $[M+Na]^+$ or $[M(^{13}C_{75})+Na]^+$ and potassiated $[M+K]^+$ or $[M(^{13}C_{75})+K]^+$. Brackets below the panels denote signals corresponding to [^{13}C]-enriched Dols in indicated cationic forms.

(D) and (E) – arrows indicate signals corresponding to monoisotopic [^{1}H]- and expected precursor-specific maximally deuterium-labeled Dol-15 ions: protonated $[M(^{2}H_{30})+H]^+$ or $[M(^{2}H_{15})+H]^+$, ammoniated $[M(^{2}H_{30})+NH_4]^+$ or $[M(^{2}H_{15})+NH_4]^+$ and sodiated $[M(^{2}H_{30})+Na]^+$ or $[M(^{2}H_{15})+Na]^+$. Brackets below the panels denote signals corresponding to [^{2}H] enriched Dols in indicated cationic forms.

Figure 3

Mass spectra of dolichols isolated from roots fed various metabolic precursors. [U-$^{13}C_6$]glucose, [1-^{13}C]glucose, [$^{2}H_2$]deoxyxylulose ([$^{2}H_2$]DX) or [^{2}H]mevalonolactone ([^{2}H]MVL) were used in the absence or presence of sorbitol (green or blue traces, respectively). Dashed lines indicate the *m/z* of signals assigned to monoisotopic ions of ammoniated, sodiated and potassiated [$^{12}C_{5n}$]Dol-n.

Please note that the *m/z* axis is adjusted to the value of the molecular mass (M) of monoisotopic [$^{12}C_{5n}$]Dol-n for each Dol-n.

Figure 4

Correlation of signal intensities of cationic adducts, ammoniated $[M+NH_4]^+$ vs. sodiated $[M+Na]^+$, for monoisotopic [$^{12}C_{5n}$]Dol-n ions of each Dol-n species (for explanation see Fig. 2 for Dol-15). Shown are data obtained after labeling from [U-$^{13}C_6$]glucose. Please note that such analysis was not possible for ^{13}C-enriched ammoniated and sodiated Dol-n isotopomers since these distributions strongly overlapped (see Fig. 2).

Figure 5

Comparison of theoretical and experimental mass spectra obtained for labeling of Dol-15 from [U-$^{13}C_6$]glucose in control and osmotic stress conditions. Three variants of the theoretical envelopes were calculated for both control (A,B,C) and osmotic stress (D,E,F) conditions. It was assumed that the isotopic enrichment of [^{13}C]Dol-15 was 99% (A,D), i.e., it was synthesized from [U-$^{13}C_6$]glucose (99% ^{13}C isotopic abundance) as the sole source of carbon; 93.9 ± 1.0% (B) and 80.7 ± 1.3% (E) to account for some dilution with endogenous native glucose (~1% ^{13}C isotopic abundance); alternatively, labeling from [U-$^{13}C_6$]glucose together with an additional involvement of native IPP was considered: 96.1% [U-$^{13}C_6$]glucose and 2.8% native IPP (final isotopic enrichment of Dol-15 was 93.9 ± 1.0%) (C) or 87.4% [U-$^{13}C_6$]glucose and 8.5% native IPP (final isotopic enrichment of Dol-15 was 80.7 ± 1.3%) (F). Green and blue traces represent the experimental spectra recorded in control and osmotic stress conditions, respectively, while red – the theoretical ones.

Vertical lines indicate the *m/z* of the cationic, ammoniated ($[M+NH_4]^+$ and $[M(^{13}C_{75})+NH_4]^+$, and sodiated ($[M+Na]^+$ and $([M(^{13}C_{75})+Na]^+$ forms of the respective monoisotopic ions {[$^{12}C_{75}$]Dol-15 - solid and [$^{13}C_{75}$]- dotted}.

Figure 6

^{13}C enrichment profiles of Dol-14 -23 metabolically labeled from [U-$^{13}C_6$]glucose in the absence (dotted lines – control) or presence (solid lines) of sorbitol represented as cumulative isotopomer distributions (CDF) directly derived from mass spectra. Overlaid CDFs are presented for all analyzed Dol-n as well as for selected Dol-14, -17, -20 and -23. For each Dol-n the differences between sorbitol-treated vs. control roots are statistically significant ($\alpha < 10^{-5}$) according to the Mann-Whitney test applied for pairs of CDFs of respective Dol.

Please note that the *m/z* axis is adjusted to the value of (M) for each respective Dol-n.

Figure 7

Comparison of theoretical and experimental mass spectra obtained for labeling of Dol-15 and Dol-20 from [1-^{13}C]glucose in control and the osmotic stress conditions. Three variants of the theoretical spectra were calculated for both control (A,B,C and A',B',C' for Dol-15 and Dol-20, respectively) and osmotic stress (D,E,F and D',E',F') conditions assuming that [^{13}C]Dols were synthesized solely via the MEP (A,D and A',D') or the MVA (B,E and B',E') pathway, or with a contribution of the both pathways.

Green and blue traces represent the experimental spectra recorded in control and osmotic stress conditions, respectively, while red – the theoretical ones.

Vertical lines indicate the calculated *m/z* of cationic, ammoniated ($[M+NH_4]^+$, sodiated ($[M+Na]^+$) and potassiated ($[M+K]^+$) forms of monoisotopic [$^{12}C_{75}$]Dol-15 and [$^{12}C_{100}$]Dol-20 ions.

Figure 8

Figure 8A

Mass spectra of phytosterols isolated from roots fed various metabolic precursors: [U-$^{13}C_6$]glucose, [1-^{13}C]glucose, [$^2H_2$]deoxyxylulose (DX) or [^{2}H]mevalonolactone (MVL) in the absence or presence of sorbitol (green or blue bars, respectively). For labeling with [1-

865 ^{13}C]glucose three theoretical isotopic envelopes of the mass spectra are presented for each
866 phytosterol calculated with the assumption that the phytosterol originates exclusively from
867 either the MEP or MVA pathway (dotted or dashed line, respectively), or from both (bold).
868 Please note that the *m/z* axis is adjusted to the value of the molecular mass (M) of the
869 respective monoisotopic [^{12}C]phytosterol. For consistency only the fragments of the mass
870 spectra containing signals corresponding to the molecular ions of [^{13}C]phytosterol are
871 presented for labeling with [U-$^{13}C_6$]glucose.

872 **Figure 8B**

873 **Theoretical mass distributions (isotopic envelopes) estimated for phytosterols** synthesized
874 from [1-^{13}C]glucose solely via the MEP or the MVA pathway (red and blue line, respectively)
875 are represented by binomial distributions with 10 or 15 tries and p=0.5.

876 **Figure 9**

877 **Osmotic stress modulates input of MEP and MVA pathways to dolichol synthesis.**
878 Biosynthetic origins of Dol-16 (and other dominating dolichols, Dol-14, -15 and -17) changes
879 upon osmotic stress while that of Dol-21 (and other long-chain Dols, n>18 and also Dol-13)
880 remains unaffected. This implies that upon osmotic stress the oligoprenyl precursors
881 synthesized by plastidial *cis*-prenyltransferase (CPT) and translocated to the cytoplasm are
882 longer than those synthesized in control conditions. In contrast, the synthesis of long-chain
883 Dols proceeds most probably in a cellular compartment other than plastids/cytoplasm. Such
884 activity is tentatively assigned to peroxisomal CPT which most probably utilizes an
885 autonomous, MVA-dependent, pool of IPP in concert with MEP-derived IPP imported to
886 peroxisomes through plastid-peroxisome contact sites (Shai et al., 2016). Modulation of the
887 intensity of export of plastidial MEP-derived IPP and possibly oligoprenyl diphosphates upon
888 stress is depicted by cyan and white arrows, respectively.

889

SUPPLEMENTAL DATA

Supplementary Figure 1. Effect of cadmium chloride on expression level of *CPTs* in Arabidopsis hairy roots

Supplementary Figure 2. Effect of oxidative stress on: (A) expression level of *CPTs* in Arabidopsis hairy roots; (B) level of MDA.

Supplementary Figure 3. Experimental and theoretical spectra of [^{13}C]Dol-n after feeding [U-$^{13}C_6$]glucose (two leftmost columns) or [1-^{13}C]glucose (two rightmost columns).

Supplementary Figure 4. Estimated number of MVA-derived isoprene units (i.u.) in various Dol-n synthesized in control (diamonds) or osmotic stress (triangles) conditions (related to Table 2).

Supplementary Figure 5. Comparison of theoretical mass spectra of Dol-20 calculated for the MEP (orange) and MVA (magenta) pathways.

Supplementary Figure 1

Effect of cadmium chloride on expression level of *CPTs* in Arabidopsis hairy roots

Supplementary Figure 2

Effect of oxidative stress on: (A) expression level of *CPTs* in Arabidopsis hairy roots; (B) level of MDA.

Supplementary Figure 3

Experimental and theoretical spectra of [^{13}C]Dol-n after feeding [U-$^{13}C_6$]glucose (two leftmost columns) or [1-^{13}C]glucose (two rightmost columns). Theoretical spectra are shown in red, experimental in green (control) or blue (osmotic stress).

913 **[U-$^{13}C_6$]glucose**: comparison of the theoretical spectra with experimental ones allowed
914 calculation of the effective ^{13}C abundance of 93.9 ± 1.0% under control conditions and 80.7 ±
915 1.3% under osmotic stress;
916 **[1-^{13}C]glucose**: comparison of the theoretical spectra with experimental ones allowed
917 calculation of the contribution of the MEP and MVA pathways to Dol biosynthesis.
918 Dotted lines indicate the *m/z* of ammoniated ($[M+NH_4]^+$), sodiated ($[M+Na]^+$) and potassiated
919 ($[M+K]^+$) ions of monoisotopic [$^{12}C_{5n}$]Dol-n.
920 Please note that the *m/z* axis is adjusted to the value of (M) for each respective Dol-n.
921 **Supplementary Figure 4**
922 Estimated number of MVA-derived isoprene units (i.u.) in various Dol-n synthesized in
923 control (diamonds) or osmotic stress (triangles) conditions (related to Table 2).
924 Contribution of the MVA pathway to Dol-n biosynthesis is substantially decreased for Dol-14
925 -17 in the stress conditions. The metabolic origin of longer-chain Dols (Dol-18 – 21) is
926 unaffected by sorbitol.
927 **Supplementary Figure 5**
928 Comparison of theoretical mass spectra of Dol-20 calculated for the MEP (orange) and MVA
929 (magenta) pathways obtained from labeling with either [1-^{13}C]glucose or [1,6-$^{13}C_2$]glucose
930 (left and right column, respectively) of various isotopic ^{13}C abundance (95, 80, 25, 10%);
931 shown are protonated $[M+H]^+$ ions.
932

Table 1. Content of dolichols, polyprenols and phytosterols in Arabidopsis hairy roots exposed to various stress factors. Dol, Pren and phytosterol content was estimated using, respectively, HPLC/UV and GC/FID, n,=3, results significantly ($p<0.05$) different from the control are indicated.

t-BHP and MV stand for *tert*-butyl hydroperoxide and methyl viologen, respectively.

Stress		Dolichol content [µg/g FW]	Fraction of dominating Dolichols (D-14 - D-17) in total Dol mixture % ± SD	Fraction of Polyprenols (P-14 - P-17) in total Pren mixture % ± SD	Phytosterol content [mg/g FW]
osmotic sorbitol [M]	control	4.4 ± 0.6	67 ± 7	15 ± 1	2.1 ± 0.4
	0.2	4.9 ± 0.6	76 ± 9	22 ± 2	1.9 ± 0.3
	0.3	**6.4*** ± 0.6	91 ± 8	36 ± 3	1.9 ± 0.5
	0.4	**6.9*** ± 0.4	93 ± 9	35 ± 3	1.9 ± 0.7
	0.5	**6.5*** ± 0.1	88 ± 5	38 ± 4	1.9 ± 0.6
oxidative	control	4.4 ± 0.2	66 ± 3	14 ± 2	2.0 ± 0.6
	1 mM H_2O_2	**5.3*** ± 0.3	81 ± 4	23 ± 2	1.9 ± 0.2
	0.3 mM *t*-BHP	**5.8*** ± 0.6	88 ± 5	26 ± 2	**5.2*** ± 0.4
	1 µM MV	4.0 ± 0.2	61 ± 7	12 ± 1	**4.0*** ± 0.6
$CdCl_2$ [µM]	control	4.4 ± 0.5	67 ± 7	15 ± 2	2.0 ± 0.3
	25	**5.6*** ± 0.3	86 ± 8	27 ± 2	2.3 ± 0.3
	50	**6.6*** ± 0.6	91 ± 4	28 ± 2	2.0 ± 0.3

938 * differs from the control at $p<0.05$

939 **Table 2. Number of MEP- and MVA-derived isoprene units in Dol-n molecule**

940 **synthesized in control and stress conditions.**

941 Dols were isolated from Arabidopsis hairy roots fed [1-^{13}C]glucose upon control and stress

942 conditions. n_{MEP} and n_{MVA} stand for the number of MEP- and MVA-derived isoprene units,

943 respectively, $n=n_{MEP}+n_{MVA}$.

944 All n_{MEP} values from the estimated ranges shown give almost equivalent models (according to

945 chi-square test) for each Dol-n.

	Control		Sorbitol	
	n_{MEP}	n_{MVA}	n_{MEP}	n_{MVA}
Dol-13	8-9	4-5	9	4
Dol-14	11-12	2-3	14	0
Dol-15	8-11	4-7	15	0
Dol-16	9-10	6-7	14	2
Dol-17	10-11	6-7	13-14	3-4
Dol-18	9-11	7-9	9-11	7-9
Dol-19	8-10	9-11	8-10	9-11
Dol-20	9-10	10-11	10-11	9-10
Dol-21	11-13	8-10	9-10	11-12
Dol-22	10-11	11-12	9-11	11-13
Dol-23	8-11	12-15	10-12	11-13

946

947

948 **References**

949 Abbasi AR, Hajirezaei M, Hofius D, Sonnewald U, Voll LM. 2007. Specific roles of alpha- and
950 gamma-tocopherol in abiotic stress responses of transgenic tobacco. *Plant Physiol.* **143**:1720-1738.
951 doi: 10.1104/pp.106.094771, PMID: 17293434.

952 Alex D, Bach TJ, Chye ML. 2000. Expression of *Brassica juncea* 3-hydroxy-3-methylglutaryl CoA
953 synthase is developmentally regulated and stress-responsive. *Plant J.* **22**:415-426. PMID: 10849357.

954 Bacher A, Chen F, Eisenreich W. 2016. Decoding biosynthetic pathways in plants by pulse-chase
955 strategies using $^{13}CO_2$ as a universal tracer. *Metabolites*. **6:**pii: E21. doi: 10.3390/metabo6030021,
956 PMID: 27429012.

957 Bajda A, Konopka-Postupolska D, Krzymowska M, Hennig J, Skorupinska-Tudek K, Surmacz L,
958 Wojcik J, Matysiak Z, Chojnacki T, Skorzynska-Polit E, Drazkiewicz M, Patrzylas P, Tomaszewska
959 M, Kania M, Swist M, Danikiewicz W, Piotrowska W, Swiezewska E. 2009. Role of polyisoprenoids
960 in tobacco resistance against biotic stresses. *Physiol. Plantarum* **135**:351-364. doi: 10.1111/j.1399-
961 3054.2009.01204.x, PMID: 19292825.

962 Bergamini E. 2003. Dolichol: an essential part in the antioxidant machinery of cell membranes?
963 *Biogerontology* **4**:337-339. PMID: 14756125

964 Cantagrel V, Lefeber DJ, Ng BG, Guan Z, Silhavy JL, Bielas SL, Lehle L, Hombauer H, Adamowicz
965 M, Swiezewska E, De Brouwer AP, Blümel P, Sykut-Cegielska J, Houliston S, Swistun D, Ali BR,
966 Dobyns WB, Babovic-Vuksanovic D, van Bokhoven H, Wevers RA, Raetz CR, Freeze HH, Morava
967 E, Al-Gazali L, Gleeson JG. 2010. SRD5A3 is required for converting polyprenol to dolichol and is
968 mutated in a Congenital Glycosylation Disorder. *Cell* **142**:203-217. doi: 10.1016/j.cell.2010.06.001,
969 PMID: 20637498.

970 Caretto S, Linsalata V, Colella G, Mita G, Lattanzio V. 2015. Carbon fluxes between primary
971 metabolism and phenolic pathway in plant tissues under stress. *Int J Mol Sci*. **16**:26378-
972 26394. doi: 10.3390/ijms161125967. PMID: 26556338.

973 De-Eknamkul W, Potduang B. 2003. Biosynthesis of beta-sitosterol and stigmasterol in
974 *Croton sublyratus* proceeds via a mixed origin of isoprene. *Phytochemistry* **62:**389-98. PMID:
975 12620352.

976 do Nascimento NC, Menguer PK, Henriques AT, Fett-Neto AG. 2013. Accumulation of
977 brachycerine, an antioxidant glucosidic indole alkaloid, is induced by abscisic acid, heavy metal, and
978 osmotic stress in leaves of *Psychotria brachyceras*. *Plant Physiol. Biochem.* **73**:33-40. doi:
979 10.1016/j.plaphy.2013.08.007, PMID: 24045228.

980 Ericsson J, Appelkvist EL, Thelin A, Chojnacki T, Dallner G. 1992. Isoprenoid biosynthesis in rat-
981 liver peroxisomes - characterization of *cis*-prenyltransferase and squalene synthetase. *J. Biol. Chem.*
982 **267**:18708-18714. PMID: 1527001.

983 Ettenhuber C, Radykewicz T, Kofer W, Koop HU, Bacher A, Eisenreich W. 2005. Metabolic flux
984 analysis in complex isotopolog space. Recycling of glucose in tobacco plants. *Phytochemistry*
985 **66**:323-335. PMID: 15680989.

986 Ge XC, Wu JY. 2005. Tanshinone production and isoprenoid pathways in *Salvia miltiorrhiza* hairy
987 roots induced by Ag^{+} and yeast elicitor. *Plant Sci.* **168**:487-491. doi:10.1016/j.plantsci.2004.09.012.

988 Gruchattka E, Haedicke O, Klamt S, Schuetz V, Kayser O. 2013. In silico profiling of *Escherichia*
989 *coli* and *Saccharomyces cerevisiae* as terpenoid factories. *Microb. Cell Fact.* **12**:84. doi:
990 10.1186/1475-2859-12-84, PMID: 24059635.

991 Heath RL, Packer L. 1968. Photoperoxidation in isolated chloroplasts. I. Kinetics and stoichiometry
992 of fatty acid peroxidation. *Arch. Biochem. Biophys.* **125**:189-198. PMID: 5655425.

993 Hemmerlin A, Bach TJ. 2000. Farnesol-induced cell death and stimulation of 3-hydroxy-3-

994 methylglutaryl-coenzyme A reductase activity in tobacco cv Bright Yellow-2 cells. *Plant Physiol.*
995 **123**:1257-1268. PMID: 10938345.

996 Hemmerlin A, Harwood JL, Bach TJ. 2012. A raison d'etre for two distinct pathways in the early
997 steps of plant isoprenoid biosynthesis? *Prog. Lipid Res.* **51**:95-148. doi:
998 10.1016/j.plipres.2011.12.001, PMID: 22197147.

999 Huang GT, Ma SL, Bai LP, Zhang L, Ma H, Jia P, Liu J, Zhong M, Guo ZF. 2012. Signal
1000 transduction during cold, salt, and drought stresses in plants. *Mol. Biol. Rep.* **39**:969-987. doi:
1001 10.1007/s11033-011-0823-1, PMID: 21573796.

1002 Jozwiak A, Gutkowska M, Gawarecka K, Surmacz L, Buczkowska A, Lichocka M, Nowakowska J,
1003 Swiezewska E. 2015. POLYPRENOL REDUCTASE2 deficiency is lethal in Arabidopsis due to male
1004 sterility. *Plant Cell* **27**:3336-53. doi: 10.1105/tpc.15.00463, PMID: 26628744.

1005 Jozwiak A, Ples M, Skorupinska-Tudek K, Kania M, Dydak M, Danikiewicz W, Swiezewska E.
1006 2013. Sugar availability modulates polyisoprenoid and phytosterol profiles in *Arabidopsis thaliana*
1007 hairy root culture. *Biochim. Biophys. Acta* **1831**:438-47. doi: 10.1016/j.bbalip.2012.11.006, PMID:
1008 23178167.

1009 Keller RK. 1986. The mechanism and regulation of dolichyl phosphate biosynthesis in rat-liver. *J.*
1010 *Biol. Chem.* **261**:2053-2059. PMID: 3638306.

1011 Kera K, Takahashi S, Sutoh T, Koyama T, Nakayama T. 2012. Identification and characterization of
1012 a *cis*, *trans*-mixed heptaprenyl diphosphate synthase from *Arabidopsis thaliana*. *FEBS J*. **279**:3813–
1013 3827. PMID: 2883514.

1014 Krasensky J, Jonak C. 2012. Drought, salt, and temperature stress-induced metabolic rearrangements
1015 and regulatory networks. *Journal of Experimental Botany* **63**:1593-1608. doi: 10.1093/jxb/err460,
1016 PMID: 22291134.

1017 Lin YF, Aarts MGM. 2012. The molecular mechanism of zinc and cadmium stress response in plants.

Cell. Mol. Life Sci. **69**:3187-3206. doi: 10.1007/s00018-012-1089-z, PMID: 22903262.

Lipko A, Swiezewska E. 2016. Isoprenoid generating systems in plants — A handy toolbox how to assess contribution of the mevalonate and methylerythritol phosphate pathways to the biosynthetic process. *Prog. Lipid Res.* **63**:70-92. doi: 10.1016/j.plipres.2016.04.002, PMID: 27133788.

Mansouri H, Asrar Z, Mehrabani M. 2009. Effects of gibberellic acid on primary terpenoids and delta(9)-tetrahydrocannabinol in *Cannabis sativa* at flowering stage. *J. Integ. Plant Biol.* **51**:553-561. doi: 10.1111/j.1744-7909.2009.00833.x, PMID: 19522814.

Marquardt DW. 1963. An algorithm for least-squares estimation of nonlinear parameters. *J. Soc. Industr. App. Mathem.* **11**:431-441.

Maurel K, Sakr S, Gerbe F, Guilliot A, Bonhomme M, Rageau R, Pétel G. 2004. Sorbitol uptake is regulated by glucose through the hexokinase pathway in vegetative peach-tree buds. *J. Exp. Bot.* **55**:879-888. doi: 10.1093/jxb/erh087, PMID: 14990620.

May B, Lange BM, Wuest M. 2013. Biosynthesis of sesquiterpenes in grape berry exocarp of *Vitis vinifera* L.: Evidence for a transport of farnesyl diphosphate precursors from plastids to the cytosol. *Phytochemistry* **95**:135-144. doi: 10.1016/j.phytochem.2013.07.021, PMID: 23954075.

Meier S, Tzfadia O, Vallabhaneni R, Gehring C, Wurtzel ET. 2011. A transcriptional analysis of carotenoid, chlorophyll and plastidial isoprenoid biosynthesis genes during development and osmotic stress responses in *Arabidopsis thaliana*. *BMC Systems Biol.* **5**:19. doi: 10.1186/1752-0509-5-77, PMID: 21595952.

Meyer O, Hoeffler JF, Grosdemange-Billiard C, Rohmer M. 2004. Practical synthesis of 1-deoxy-D-xylulose and 1-deoxy-d-xylulose 5-phosphate allowing deuterium labeling. *Tetrahedron*; **60**:12153–12162. doi:10.1016/j.tet.2004.10.016.

Moremen KW, Tiemeyer M, Nairn AV. 2012. Vertebrate protein glycosylation: diversity, synthesis and function. *Nat. Rev. Mol. Cell Biol.* **13**:448–462. PMID: 22722607.

1042 Moreno AA, Orellana A. 2011. The physiological role of the unfolded protein response in plants.
1043 *Biol. Res.* **44**:75-80. doi: 10.4067/S0716-97602011000100010, PMID: 21720684.

1044 Nagegowda DA, Ramalingam S, Hemmerlin A, Bach TJ, Chye ML. 2005. *Brassica juncea* HMG-
1045 CoA synthase: localization of mRNA and protein. *Planta* **221**:844-856. doi: 10.1007/s00425-005-
1046 1497-5, PMID: 15770484.

1047 Obata T, Fernie AR. 2012. The use of metabolomics to dissect plant responses to abiotic stresses.
1048 *Cell. Mol. Life Sci.* **69**:3225-3243. doi: 10.1007/s00018-012-1091-5, PMID: 22885821.

1049 Opitz S, Nes WD, Gershenzon J. 2014. Both methylerythritol phosphate and mevalonate pathways
1050 contribute to biosynthesis of each of the major isoprenoid classes in young cotton seedlings.
1051 *Phytochemistry* **98**:110-119. doi: 10.1016/j.phytochem.2013.11.010, PMID: 24359633.

1052 Pokhilko A, Bou-Torrent J, Pulido P, Rodríguez-Concepción M, Ebenhöh O. 2015. Mathematical
1053 modelling of the diurnal regulation of the MEP pathway in Arabidopsis. *New Phytol*. 206:1075-1085.
1054 doi: 10.1111/nph.13258. PMID: 25598499.

1055 Pulido P, Perello C, Rodriguez-Concepcion M. 2012. New insights into plant isoprenoid metabolism.
1056 *Mol. Plant* **5**:964-967. doi: 10.1093/mp/sss088, PMID: 22972017.

1057 Rohmer M. 1999. The discovery of a mevalonate-independent pathway for isoprenoid biosynthesis in
1058 bacteria, algae and higher plants. *Nat. Prod. Rep.* **16**:565-574. PMID: 10584331.

1059 Schenk B, Rush JS, Waechter CJ, Aebi M. 2001. An alternative *cis*-isoprenyltransferase activity in
1060 yeast that produces polyisoprenols with chain lengths similar to mammalian dolichols. *Glycobiology*
1061 **11**:89-98. PMID: 11181565.

1062 Schuhr CA, Radykevicz T, Sagner S, Latzel C, Zenk MH, Arigoni D, Bacher A, Rohdich F,
1063 Eisenreich W. 2003. Quantitative assessment of metabolite flux by NMR spectroscopy. Crosstalk
1064 between the two isoprenoid biosynthesis pathways in plants. *Phytochem. Rev*. **2**:3–16. doi:
1065 10.1023/B:PHYT.0000004180.25066.62.

Schwarz F, Aebi M. 2011. Mechanisms and principles of N-linked protein glycosylation. *Curr. Opin. Struct. Biol.* 21:576–582. PMID: 21978957.

Selmar D, Kleinwaechter M. 2013. Stress enhances the synthesis of secondary plant products: the impact of stress-related over-reduction on the accumulation of natural products. *Plant Cell Physiol.* **54**:817-826. doi: 10.1093/pcp/pct054, PMID: 23612932.

Shai N, Schuldiner M, Zalckvar E. 2016. No peroxisome is an island - Peroxisome contact sites. *Biochim. Bophys. Acta* **1863**:1061-1069. doi: 10.1016/j.bbamcr.2015.09.016, PMID: 26384874.

Sharma R, De Vleesschauwer D, Sharma MK, Ronald PC. 2013. Recent advances in dissecting stress-regulatory crosstalk in rice. *Mol. Plant* **6**:250-260. doi: 10.1093/mp/sss147, PMID: 23292878.

Simkin AJ, Guirimand G, Papon N, Courdavault V, Thabet I, Ginis O, Bouzid S, Giglioli-Guivarc'h N, Clastre M. 2011. Peroxisomal localisation of the final steps of the mevalonic acid pathway *in planta*. *Planta* **234**:903-914. doi: 10.1007/s00425-011-1444-6, PMID: 21655959.

Skoneczny M, Kludkiewicz B, Swiezewska E, Szkopinska A. 2006. Activity of *Pichia pastoris* alternative *cis*-prenyltransferase is correlated with proliferation of peroxisomes. *Cell Biol. Int.* **30**:122-6. doi: 10.1016/j.cellbi.2005.09.006, PMID: 16271301.

Skorupinska-Tudek K, Bieńkowski T, Olszowska O, Furmanowa M, Chojnacki T, Danikiewicz W, Swiezewska E. 2003. Divergent pattern of polyisoprenoid alcohols in the tissues of *Coluria geoides*: a new electrospray ionization MS approach. *Lipids*. **38**:981-90. PMID: 14584606.

Skorupinska-Tudek K, Poznanski J, Wojcik J, Bienkowski T, Szostkiewicz I, Zelman-Femiak M, Bajda A, Chojnacki T, Olszowska O, Grunler J, Meyer O, Rohmer M, Danikiewicz W, Swiezewska E. 2008. Contribution of the mevalonate and methylerythritol phosphate pathways to the biosynthesis of dolichols in plants. *J. Biol. Chem.* **283**:21024-21035. doi: 10.1074/jbc.M706069200, PMID: 18502754.

1090 Strasser R. 2016. Plant protein glycosylation. *Glycobiology* **26**:926-939. doi:
1091 10.1093/glycob/cww023, PMID: 26911286.

1092 Surmacz L, Plochocka D, Kania M, Danikiewicz W, Swiezewska E. 2014. *cis*-
1093 Prenyltransferase AtCPT6 produces a family of very short-chain polyisoprenoids *in planta*.
1094 *Biochim. Biophys. Acta* **1841**:240-250. doi: 10.1016/j.bbalip.2013.11.011, PMID: 24291644.

1095 Surmacz L, Swiezewska E. 2011. Polyisoprenoids - Secondary metabolites or physiologically
1096 important superlipids? *Biochem. Biophys. Res. Comm.* **407**:627-632. doi: 10.1016/j.bbrc.2011.03.059,
1097 PMID: 21419101.

1098 Swiezewska E, Danikiewicz W. 2005. Polyisoprenoids: structure, biosynthesis and function. *Prog.*
1099 *Lipid Res*. **44**:235-258. PMID: 16019076.

1100 Thompson SL, Burrows R, Laub RJ, Krisans SK. 1987. Cholesterol synthesis in rat liver
1101 peroxisomes. Conversion of mevalonic acid to cholesterol. *J. Biol. Chem.* **262**:17420-17425.
1102 PMID: 3693362.

1103 Valentovic P, Luxova M, Kolarovic L, Gasparikova O. 2006. Effect of osmotic stress on
1104 compatible solutes content, membrane stability and water relations in two maize cultivars.
1105 *Plant Soil Envir*. **52**:186-191.

1106 Walley J, Xiao Y, Wang JZ, Baidoo EE, Keasling JD, Shen Z, Briggs SP, Dehesh K. 2015. Plastid-
1107 produced interorgannellar stress signal MEcPP potentiates induction of the unfolded protein response
1108 in endoplasmic reticulum. *Proc. Natl Acad. Sci. USA* **112**:6212-6217. doi: 10.1073/pnas.1504828112,
1109 PMID: 25922532.

1110 Wu SJ, Shi M, Wu JY. 2009. Cloning and characterization of the 1-deoxy-D-xylulose 5-phosphate
1111 reductoisomerase gene for diterpenoid tanshinone biosynthesis in *Salvia miltiorrhiza* (Chinese sage)
1112 hairy roots. *Biotech. Appl. Biochem.* **52**:89-95. doi: 10.1042/BA20080004, PMID: 18302535.

1113 Xiao Y, Savchenko T, Baidoo EE, Chehab WE, Hayden DM, Tolstikov V, Corwin JA, Kliebenstein

1114 DJ, Keasling JD, Dehesh K. 2012. Retrograde signaling by the plastidial metabolite MEcPP regulates
1115 expression of nuclear stress-response genes. *Cell* **149**:1525-1535. doi: 10.1016/j.cell.2012.04.038,
1116 PMID: 22726439.

1117 Yan X, Zhang L, Wang J, Liao P, Zhang Y, Zhang R, Kai G. 2009. Molecular characterization and
1118 expression of 1-deoxy-d-xylulose 5-phosphate reductoisomerase (DXR) gene from *Salvia*
1119 *miltiorrhiza*. *Acta Phys. Plant.* **31**:1015-1022. doi:10.1007/s11738-009-0320-5.

1120 Yang D, Du X, Liang X, Han R, Liang Z, Liu Y, Liu F, Zhao J. 2012. Different roles of the
1121 mevalonate and methylerythritol phosphate pathways in cell growth and tanshinone production of
1122 *Salvia miltiorrhiza* hairy roots. *Plos One* **7**:e46797. doi: 10.1371/journal.pone.0046797, PMID:
1123 23209548.

1124

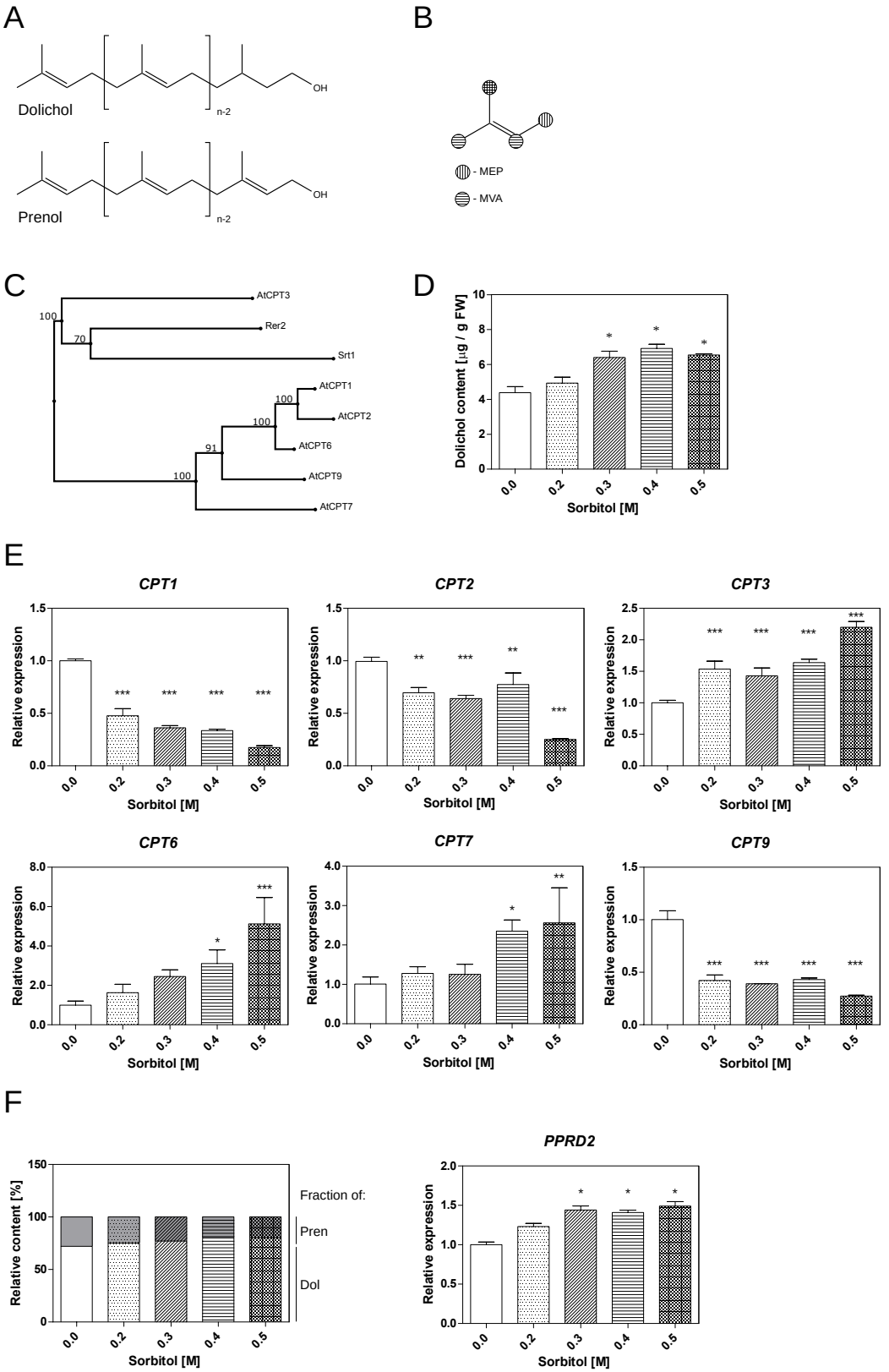

Figure 1

Polyisoprenoid alcohols of Arabidopsis hairy roots. (A) Structure of prenols and dolichols composed of n isoprene units. (B) Isoprene unit –carbon atoms potentially labeled upon feeding [1-^{13}C]glucose are marked – note different labeling pattern *via* the MEP and MVA pathways shown as vertical or horizontal striping, respectively. (C) Phylogenetic relationships among the Arabidopsis and *S. cerevisiae cis*-prenyltransferases (Rer2 and Srt1) were reconstructed using a multiple sequence alignment program, MAFFT (http://mafft.cbrc.jp/) with L-INS-i alignment method. CPTs from *S. cerevisiae*: Rer2 and Srt1 (P35196 and Q03175) and *A. thaliana*: AtCPT1, AtCPT2, AtCPT3, AtCPT6, AtCPT7 and AtCPT9 (O80458, F4IMI8, Q8S2T1, Q8RX73, Q56Y11and Q570Q8). Effect of sorbitol on: (D) Dol accumulation, (E) relative expression of *cis*-prenyltransferases *CPTs* (RT-qPCR) and (F) left panel, relative content of dolichols and polyprenols (bars with white and gray background, respectively) and right panel, relative expression of polyprenol reductase 2 *PPRD2* in hairy roots under stress.

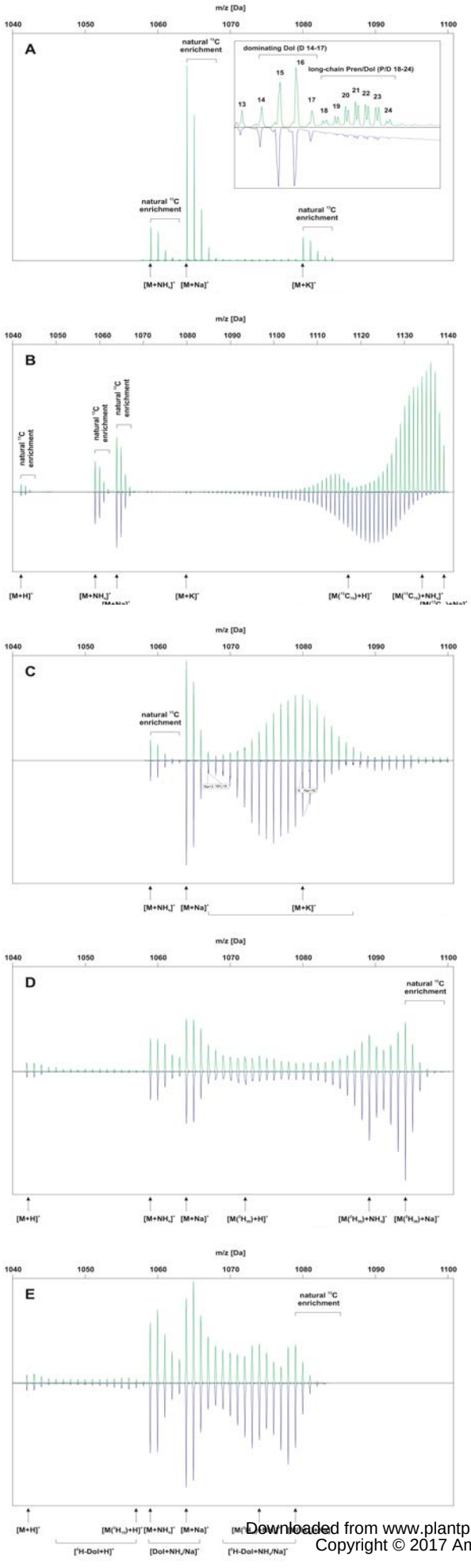

Figure 2
Mass spectra of Dol-15 metabolically labeled from various precursors applied in the absence (green trace - control) or presence of sorbitol (blue trace).

A: native Dol-15, inset presents UV spectra of polyisoprenoid mixtures isolated from roots gown in the absence or presence of sorbitol (green or blue trace, respectively). Signals corresponding to the analyzed Dol families (dominating Dols and long-chain Dols) are indicated.

B: feeding [U-$^{13}C_6$]glucose

C: feeding [1-^{13}C]glucose

D: feeding [$^2H_2$]deoxyxylulose

E: feeding [^{2}H]mevalonolactone

M is the *m/z* of monoisotopic [$^{12}C_{75}$]Dol-15. Brackets above the spectra indicate signals of [^{13}C]Dol-15 isotopomers synthesized from precursors with natural [^{13}C] abundance.

(B) and (C) - arrows indicate signals corresponding to monoisotopic [$^{12}C_{75}$]- and [$^{13}C_{75}$]Dol-15 ions: protonated [M+H]$^+$ or [M($^{13}C_{75}$)+H]$^+$, ammoniated [M+NH$_4$]$^+$ or [M($^{13}C_{75}$)+NH$_4$]$^+$, sodiated [M+Na]$^+$ or [M($^{13}C_{75}$)+Na]$^+$ and potassiated [M+K]$^+$ or [M($^{13}C_{75}$)+K]$^+$. Brackets below the panels denote signals corresponding to [^{13}C]-enriched Dols in indicated cationic forms.

(D) and (E) – arrows indicate signals corresponding to monoisotopic [^{1}H]- and expected precursor-specific maximally deuterium-labeled Dol-15 ions: protonated [M($^2H_{30}$)+H]$^+$ or [M($^2H_{15}$)+H]$^+$, ammoniated [M($^2H_{30}$)+NH$_4$]$^+$ or [M($^2H_{15}$)+NH$_4$]$^+$ and sodiated [M($^2H_{30}$)+Na]$^+$ or [M($^2H_{15}$)+Na]$^+$. Brackets below the panels denote signals corresponding to [^{2}H] enriched Dols in indicated cationic forms.

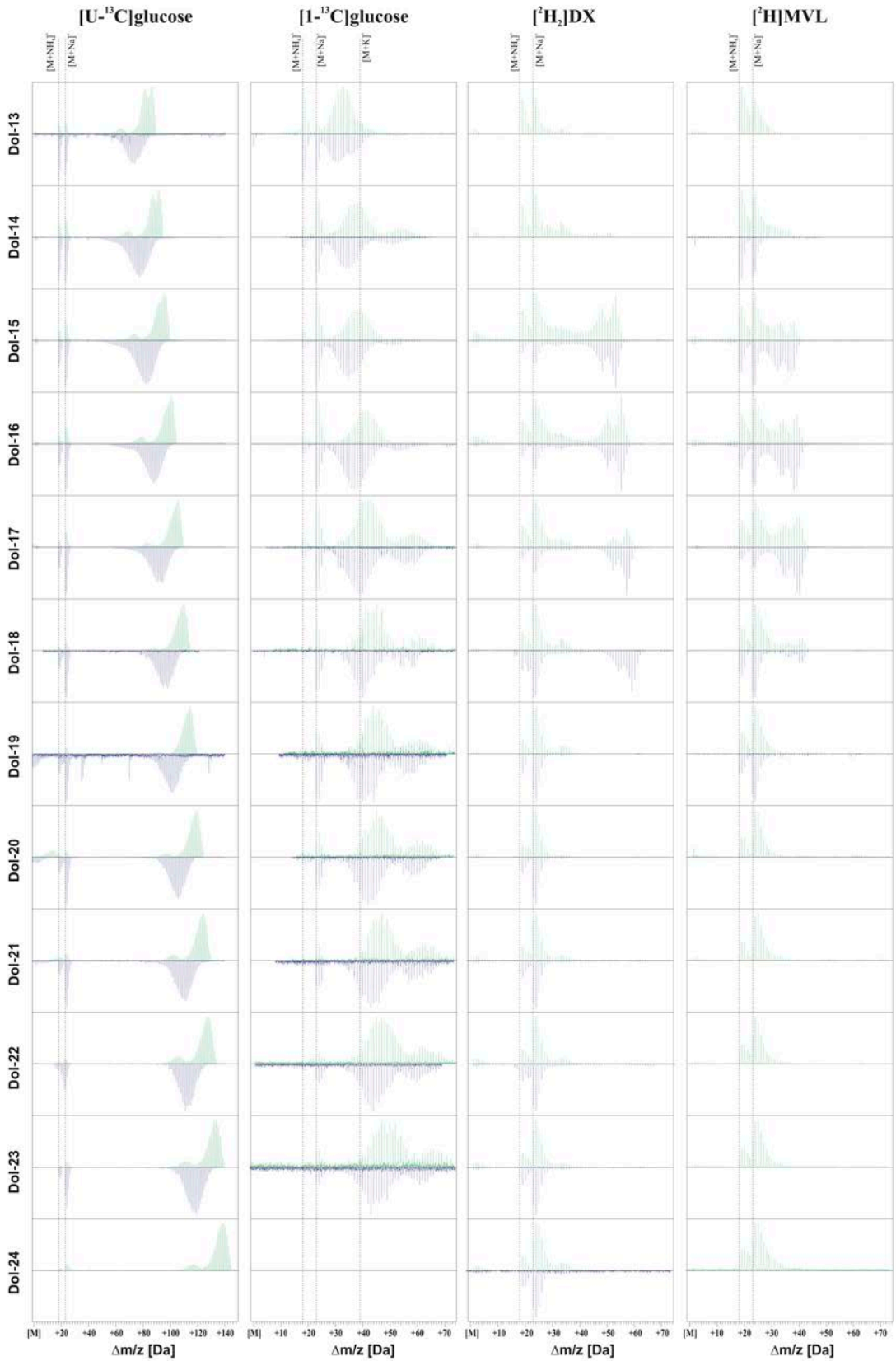

Figure 3

Mass spectra of dolichols isolated from roots fed various metabolic precursors. [U-$^{13}C_6$]glucose, [1-^{13}C]glucose, [$^2H_2$]deoxyxylulose ([$^2H_2$]DX) or [^{2}H]mevalonolactone ([^{2}H]MVL) were used in the absence or presence of sorbitol (green or blue traces, respectively). Dashed lines indicate the *m/z* of signals assigned to monoisotopic ions of ammoniated, sodiated and potassiated [$^{12}C_{5n}$]Dol-n. Please note that the *m/z* axis is adjusted to the value of the molecular mass (M) of monoisotopic [$^{12}C_{5n}$]Dol-n for each Dol-n.

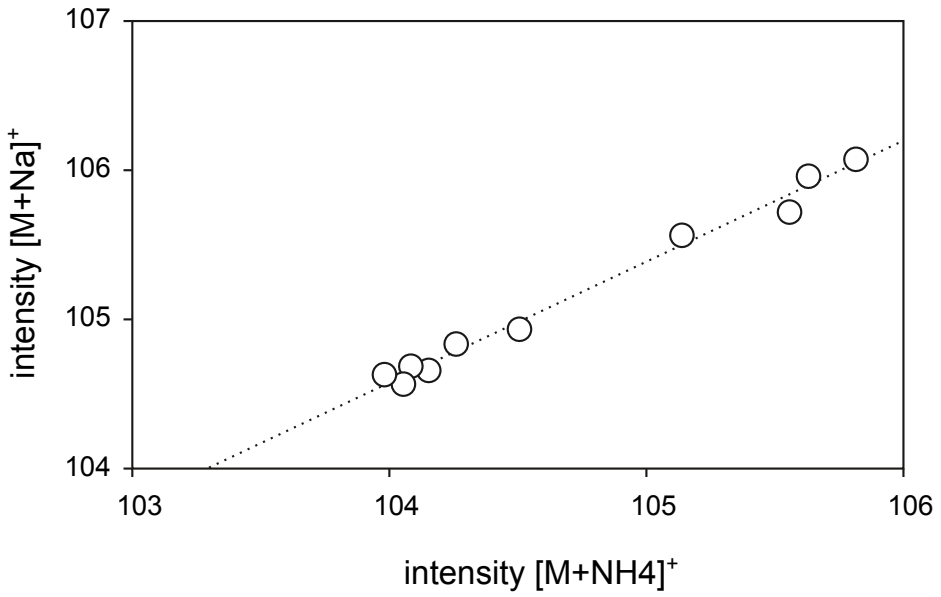

Figure 4
Correlation of signal intensities of cationic adducts, ammoniated $[M+NH_4]^+$ vs. sodiated $[M+Na]^+$, for monoisotopic $[^{12}C_{5n}]$Dol-n ions of each Dol-n species (for explanation see Fig. 2 for Dol-15). Shown are data obtained after labeling from [U-$^{13}C_6$]glucose. Please note that such analysis was not possible for ^{13}C-enriched ammoniated and sodiated Dol-n isotopomers since these distributions strongly overlapped (see Fig. 2).

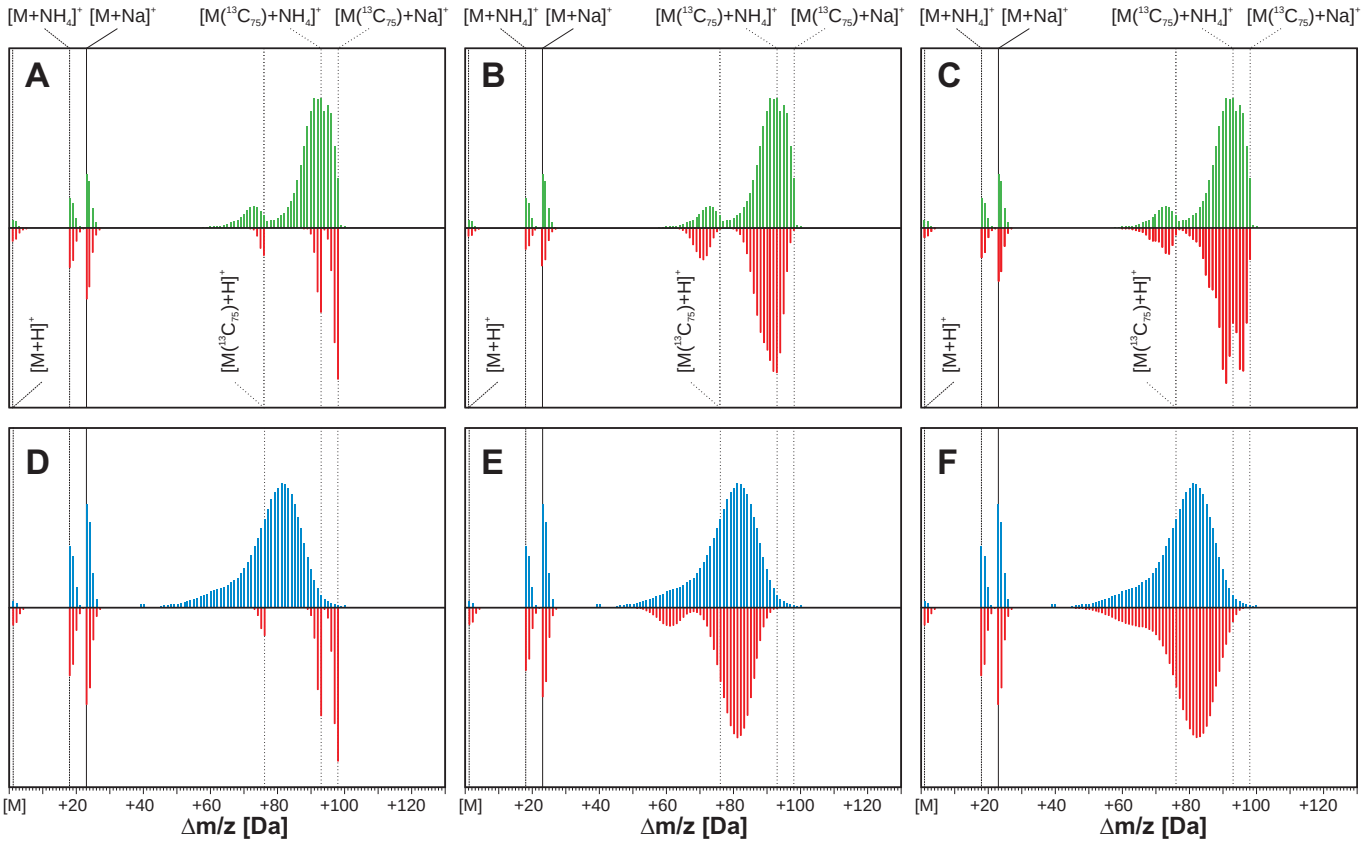

Figure 5

Comparison of theoretical and experimental mass spectra obtained for labeling of Dol-15 from [U-$^{13}C_6$]glucose in control and osmotic stress conditions. Three variants of the theoretical envelopes were calculated for both control (A,B,C) and osmotic stress (D,E,F) conditions. It was assumed that the isotopic enrichment of [^{13}C]Dol-15 was 99% (A,D), i.e., it was synthesized from [U-$^{13}C_6$]glucose (99% ^{13}C isotopic abundance) as the sole source of carbon; 93.9 ± 1.0% (B) and 80.7 ± 1.3% (E) to account for some dilution with endogenous native glucose (~1% ^{13}C isotopic abundance); alternatively, labeling from [U-$^{13}C_6$]glucose together with an additional involvement of native IPP was considered: 96.1% [U-$^{13}C_6$]glucose and 2.8% native IPP (final isotopic enrichment of Dol-15 was 93.9 ± 1.0%) (C) or 87.4% [U-$^{13}C_6$]glucose and 8.5% native IPP (final isotopic enrichment of Dol-15 was 80.7 ± 1.3%) (F).

Green and blue traces represent the experimental spectra recorded in control and osmotic stress conditions, respectively, while red – the theoretical ones.

Vertical lines indicate the *m/z* of the cationic, ammoniated ([M+NH$_4$]$^+$ and [M($^{13}C_{75}$)+NH$_4$]$^+$, and sodiated ([M+Na]$^+$ and ([M($^{13}C_{75}$)+Na]$^+$ forms of the respective monoisotopic ions {[$^{12}C_{75}$]Dol-15 - solid and [$^{13}C_{75}$]- dotted}.

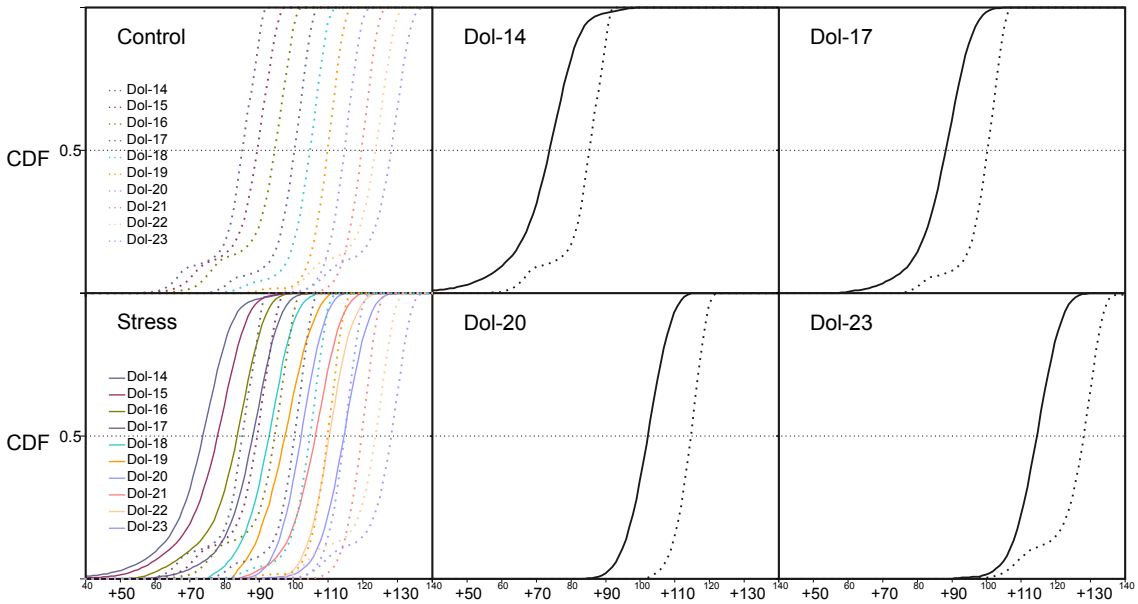

Figure 6
^{13}C enrichment profiles of Dol-14 -23 metabolically labeled from [U-$^{13}C_6$]glucose in the absence (dotted lines – control) or presence (solid lines) of sorbitol represented as cumulative isotopomer distributions (CDF) directly derived from mass spectra. Overlaid CDFs are presented for all analyzed Dol-n as well as for selected Dol-14, -17, -20 and -23.
For each Dol-n the differences between sorbitol-treated vs. control roots are statistically significant ($\alpha < 10^{-5}$) according to the Mann-Whitney test applied for pairs of CDFs of respective Dol.
Please note that the *m/z* axis is adjusted to the value of (M) for each respective Dol-n.

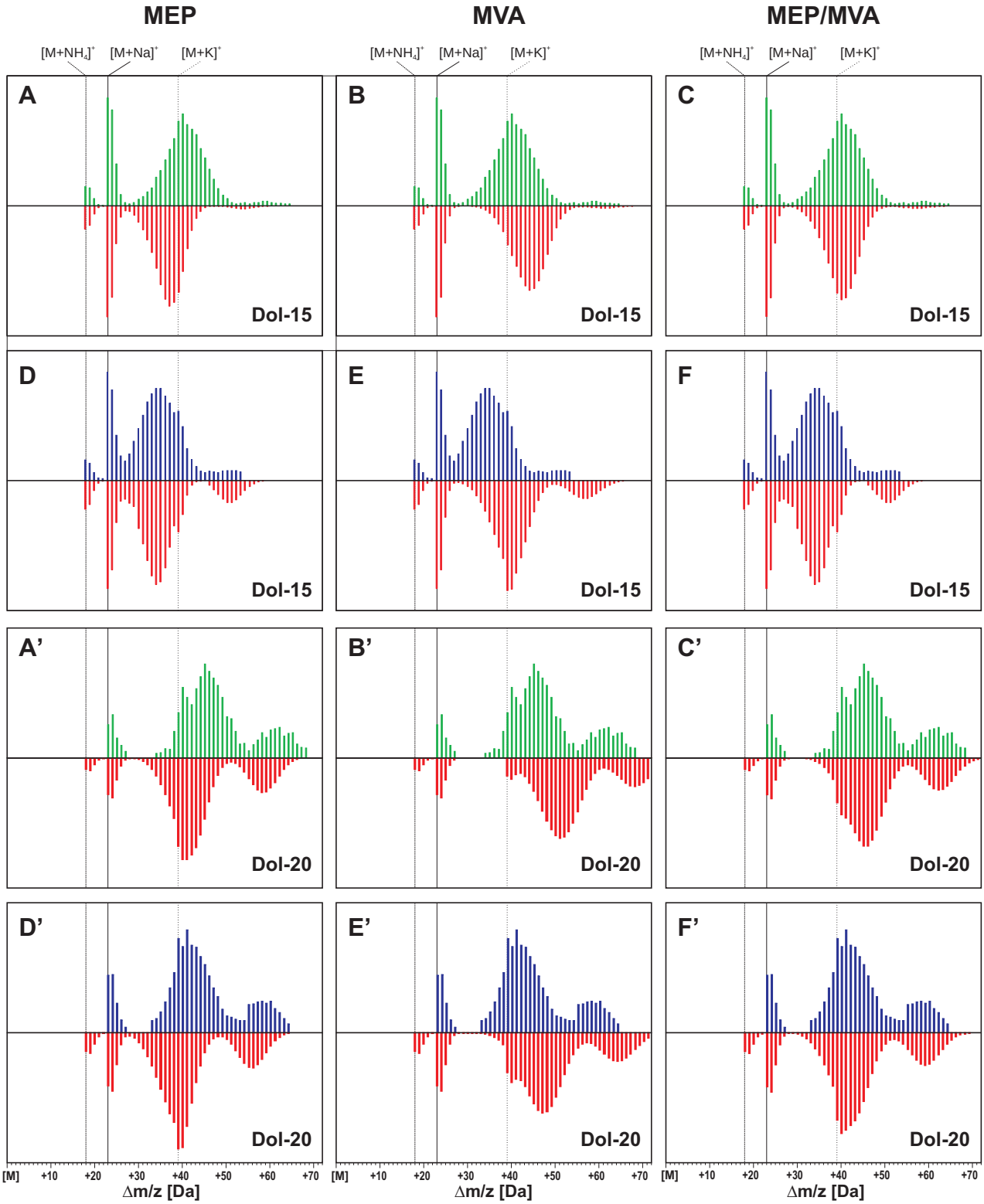

Figure 7

Comparison of theoretical and experimental mass spectra obtained for labeling of Dol-15 and Dol-20 from [1-^{13}C]glucose in control and the osmotic stress conditions.

Three variants of the theoretical spectra were calculated for both control (A,B,C and A',B',C' for Dol-15 and Dol-20, respectively) and osmotic stress (D,E,F and D',E',F') conditions assuming that [^{13}C]Dols were synthesized solely via the MEP (A,D and A',D') or the MVA (B,E and B',E') pathway, or with a contribution of the both pathways. Green and blue traces represent the experimental spectra recorded in control and osmotic stress conditions, respectively, while red – the theoretical ones. Vertical lines indicate the calculated *m/z* of cationic, ammoniated ([M+NH$_4$]$^+$, sodiated ([M+Na]$^+$) and potassiated ([M+K]$^+$) forms of monoisotopic [^{12}C$_{-}$]Dol-15 and [^{12}C$_{100}$]Dol-20 ions.

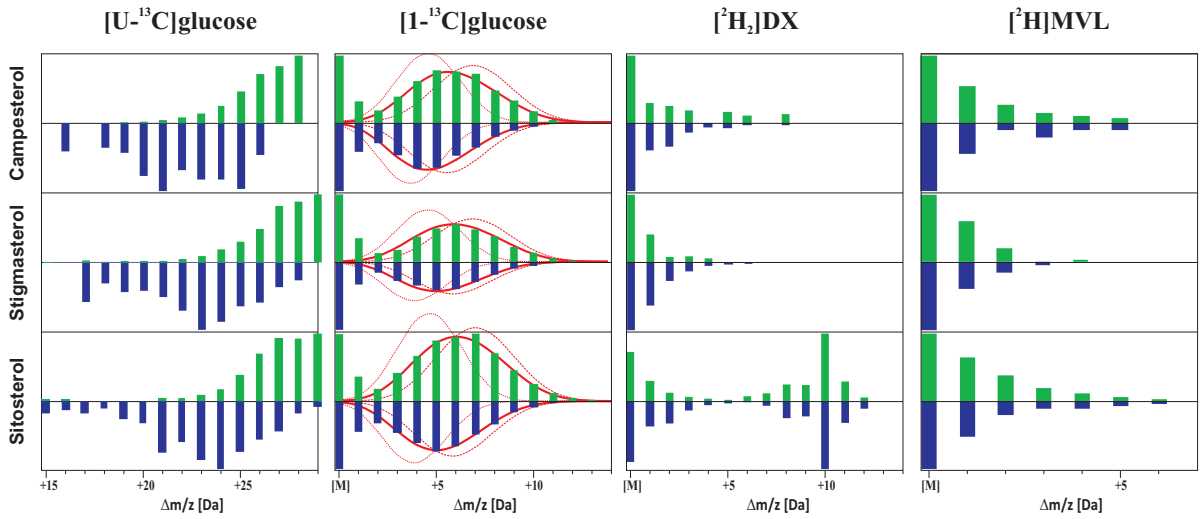

Figure 8A

Mass spectra of phytosterols isolated from roots fed various metabolic precursors: [U-$^{13}C_6$]glucose, [1-^{13}C]glucose, [$^2H_2$]deoxyxylulose (DX) or [^{2}H]mevalonolactone (MVL) in the absence or presence of sorbitol (green or blue bars, respectively). For labeling with [1-^{13}C]glucose three theoretical isotopic envelopes of the mass spectra are presented for each phytosterol calculated with the assumption that the phytosterol originates exclusively from either the MEP or MVA pathway (dotted or dashed line, respectively), or from both (bold). Please note that the *m/z* axis is adjusted to the value of the molecular mass (M) of the respective monoisotopic [^{12}C]phytosterol. For consistency only the fragments of the mass spectra containing signals corresponding to the molecular ions of [^{13}C]phytosterol are presented for labeling with [U-$^{13}C_6$]glucose.

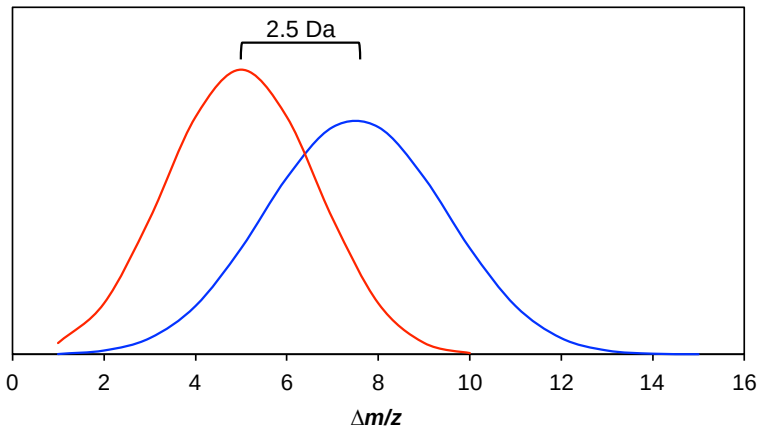

Figure 8B

Theoretical mass distributions (isotopic envelopes) estimated for phytosterols synthesized from [1-^{13}C]glucose solely via the MEP or the MVA pathway (red and blue line, respectively) are represented by binomial distributions with 10 or 15 tries and p=0.5.

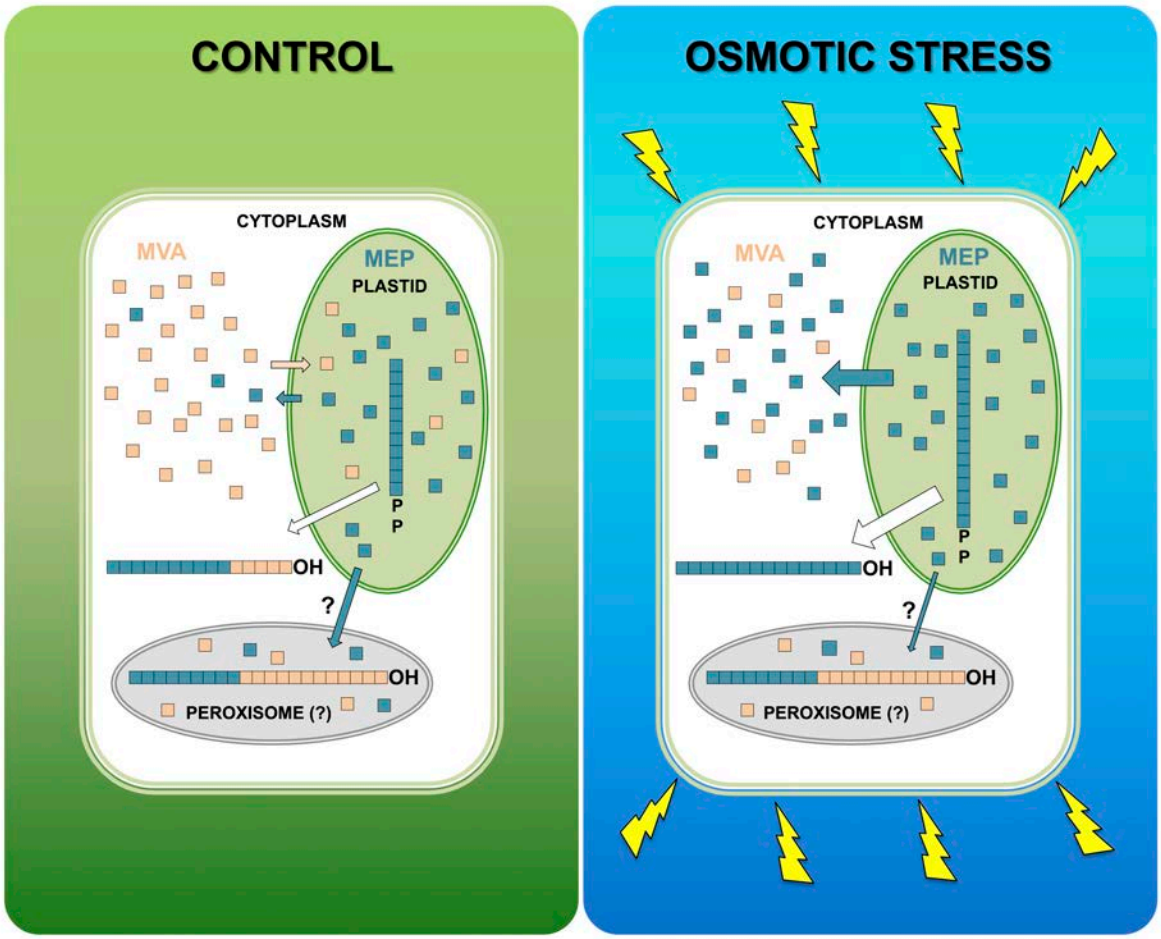

Figure 9

Osmotic stress modulates input of MEP and MVA pathways to dolichol synthesis. Biosynthetic origins of Dol-16 (and other dominating dolichols, Dol-14, -15 and -17) changes upon osmotic stress while that of Dol-21 (and other long-chain Dols, n>18 and also Dol-13) remains unaffected. This implies that upon osmotic stress the oligoprenyl precursors synthesized by plastidial *cis*-prenyltransferase (CPT) and translocated to the cytoplasm are longer than those synthesized in control conditions. In contrast, the synthesis of long-chain Dols proceeds most probably in a cellular compartment other than plastids/cytoplasm. Such activity is tentatively assigned to peroxisomal CPT which most probably utilizes an autonomous, MVA-dependent, pool of IPP in concert with MEP-derived IPP imported to peroxisomes through plastid-peroxisome contact sites (Shai et al., 2016). Modulation of the intensity of export of plastidial MEP-derived IPP and possibly oligoprenyl diphosphates upon stress is depicted by cyan and white arrows, respectively.

Parsed Citations

Abbasi AR, Hajirezaei M, Hofius D, Sonnewald U, Voll LM. 2007. Specific roles of alpha- and gamma-tocopherol in abiotic stress responses of transgenic tobacco. Plant Physiol. 143:1720-1738. doi: 10.1104/pp.106.094771, PMID: 17293434.

Pubmed: Author and Title
CrossRef: Author and Title
Google Scholar: Author Only Title Only Author and Title

Alex D, Bach TJ, Chye ML. 2000. Expression of Brassica juncea 3-hydroxy-3-methylglutaryl CoA synthase is developmentally regulated and stress-responsive. Plant J. 22:415-426. PMID: 10849357.

Pubmed: Author and Title
CrossRef: Author and Title
Google Scholar: Author Only Title Only Author and Title

Bacher A, Chen F, Eisenreich W. 2016. Decoding biosynthetic pathways in plants by pulse-chase strategies using 13CO2 as a universal tracer. Metabolites. 6:pii: E21. doi: 10.3390/metabo6030021, PMID: 27429012.

Pubmed: Author and Title
CrossRef: Author and Title
Google Scholar: Author Only Title Only Author and Title

Bajda A, Konopka-Postupolska D, Krzymowska M, Hennig J, Skorupinska-Tudek K, Surmacz L, Wojcik J, Matysiak Z, Chojnacki T, Skorzynska-Polit E, Drazkiewicz M, Patrzylas P, Tomaszewska M, Kania M, Swist M, Danikiewicz W, Piotrowska W, Swiezewska E. 2009. Role of polyisoprenoids in tobacco resistance against biotic stresses. Physiol. Plantarum 135:351-364. doi: 10.1111/j.1399-3054.2009.01204.x, PMID: 19292825.

Pubmed: Author and Title
CrossRef: Author and Title
Google Scholar: Author Only Title Only Author and Title

Bergamini E. 2003. Dolichol: an essential part in the antioxidant machinery of cell membranes? Biogerontology 4:337-339. PMID: 14756125

Pubmed: Author and Title
CrossRef: Author and Title
Google Scholar: Author Only Title Only Author and Title

Cantagrel V, Lefeber DJ, Ng BG, Guan Z, Silhavy JL, Bielas SL, Lehle L, Hombauer H, Adamowicz M, Swiezewska E, De Brouwer AP, Blümel P, Sykut-Cegielska J, Houliston S, Swistun D, Ali BR, Dobyns WB, Babovic-Vuksanovic D, van Bokhoven H, Wevers RA, Raetz CR, Freeze HH, Morava E, Al-Gazali L, Gleeson JG. 2010. SRD5A3 is required for converting polyprenol to dolichol and is mutated in a Congenital Glycosylation Disorder. Cell 142:203-217. doi: 10.1016/j.cell.2010.06.001, PMID: 20637498.

Pubmed: Author and Title
CrossRef: Author and Title
Google Scholar: Author Only Title Only Author and Title

Caretto S, Linsalata V, Colella G, Mita G, Lattanzio V. 2015. Carbon fluxes between primary metabolism and phenolic pathway in plant tissues under stress. Int J Mol Sci. 16:26378-26394. doi: 10.3390/ijms161125967. PMID: 26556338.

Pubmed: Author and Title
CrossRef: Author and Title
Google Scholar: Author Only Title Only Author and Title

De-Eknamkul W, Potduang B. 2003. Biosynthesis of beta-sitosterol and stigmasterol in Croton sublyratus proceeds via a mixed origin of isoprene. Phytochemistry 62:389-98. PMID: 12620352.

Pubmed: Author and Title
CrossRef: Author and Title
Google Scholar: Author Only Title Only Author and Title

do Nascimento NC, Menguer PK, Henriques AT, Fett-Neto AG. 2013. Accumulation of brachycerine, an antioxidant glucosidic indole alkaloid, is induced by abscisic acid, heavy metal, and osmotic stress in leaves of Psychotria brachyceras. Plant Physiol. Biochem. 73:33-40. doi: 10.1016/j.plaphy.2013.08.007, PMID: 24045228.

Pubmed: Author and Title
CrossRef: Author and Title
Google Scholar: Author Only Title Only Author and Title

Ericsson J, Appelkvist EL, Thelin A, Chojnacki T, Dallner G. 1992. Isoprenoid biosynthesis in rat-liver peroxisomes - characterization of cis-prenyltransferase and squalene synthetase. J. Biol. Chem. 267:18708-18714. PMID: 1527001.

Pubmed: Author and Title
CrossRef: Author and Title
Google Scholar: Author Only Title Only Author and Title

Ettenhuber C, Radykewicz T, Kofer W, Koop HU, Bacher A, Eisenreich W. 2005. Metabolic flux analysis in complex isotopolog space. Recycling of glucose in tobacco plants. Phytochemistry 66:323-335. PMID: 15680989.

Pubmed: Author and Title
CrossRef: Author and Title
Google Scholar: Author Only Title Only Author and Title

Ge XC, Wu JY. 2005. Tanshinone production and isoprenoid pathways in Salvia miltiorrhiza hairy roots induced by Ag+ and yeast elicitor. Plant Sci. 168:487-491. doi:10.1016/j.plantsci.2004.09.012.

Pubmed: Author and Title
CrossRef: Author and Title
Google Scholar: Author Only Title Only Author and Title

Gruchattka E, Haedicke O, Klamt S, Schuetz V, Kayser O. 2013. In silico profiling of Escherichia coli and Saccharomyces cerevisiae as terpenoid factories. Microb. Cell Fact. 12:84. doi: 10.1186/1475-2859-12-84, PMID: 24059635.
Pubmed: Author and Title
CrossRef: Author and Title
Google Scholar: Author Only Title Only Author and Title

Heath RL, Packer L. 1968. Photoperoxidation in isolated chloroplasts. I. Kinetics and stoichiometry of fatty acid peroxidation. Arch. Biochem. Biophys. 125:189-198. PMID: 5655425.
Pubmed: Author and Title
CrossRef: Author and Title
Google Scholar: Author Only Title Only Author and Title

Hemmerlin A, Bach TJ. 2000. Farnesol-induced cell death and stimulation of 3-hydroxy-3-methylglutaryl-coenzyme A reductase activity in tobacco cv Bright Yellow-2 cells. Plant Physiol. 123:1257-1268. PMID: 10938345.
Pubmed: Author and Title
CrossRef: Author and Title
Google Scholar: Author Only Title Only Author and Title

Hemmerlin A, Harwood JL, Bach TJ. 2012. A raison d'etre for two distinct pathways in the early steps of plant isoprenoid biosynthesis? Prog. Lipid Res. 51:95-148. doi: 10.1016/j.plipres.2011.12.001, PMID: 22197147.
Pubmed: Author and Title
CrossRef: Author and Title
Google Scholar: Author Only Title Only Author and Title

Huang GT, Ma SL, Bai LP, Zhang L, Ma H, Jia P, Liu J, Zhong M, Guo ZF. 2012. Signal transduction during cold, salt, and drought stresses in plants. Mol. Biol. Rep. 39:969-987. doi: 10.1007/s11033-011-0823-1, PMID: 21573796.
Pubmed: Author and Title
CrossRef: Author and Title
Google Scholar: Author Only Title Only Author and Title

Jozwiak A, Gutkowska M, Gawarecka K, Surmacz L, Buczkowska A, Lichocka M, Nowakowska J, Swiezewska E. 2015. POLYPRENOL REDUCTASE2 deficiency is lethal in Arabidopsis due to male sterility. Plant Cell 27:3336-53. doi: 10.1105/tpc.15.00463, PMID: 26628744.
Pubmed: Author and Title
CrossRef: Author and Title
Google Scholar: Author Only Title Only Author and Title

Jozwiak A, Ples M, Skorupinska-Tudek K, Kania M, Dydak M, Danikiewicz W, Swiezewska E. 2013. Sugar availability modulates polyisoprenoid and phytosterol profiles in Arabidopsis thaliana hairy root culture. Biochim. Biophys. Acta 1831:438-47. doi: 10.1016/j.bbalip.2012.11.006, PMID: 23178167.
Pubmed: Author and Title
CrossRef: Author and Title
Google Scholar: Author Only Title Only Author and Title

Keller RK. 1986. The mechanism and regulation of dolichyl phosphate biosynthesis in rat-liver. J. Biol. Chem. 261:2053-2059. PMID: 3638306.
Pubmed: Author and Title
CrossRef: Author and Title
Google Scholar: Author Only Title Only Author and Title

Kera K, Takahashi S, Sutoh T, Koyama T, Nakayama T. 2012. Identification and characterization of a cis, trans-mixed heptaprenyl diphosphate synthase from Arabidopsis thaliana. FEBS J. 279:3813-3827. PMID: 2883514.
Pubmed: Author and Title
CrossRef: Author and Title
Google Scholar: Author Only Title Only Author and Title

Krasensky J, Jonak C. 2012. Drought, salt, and temperature stress-induced metabolic rearrangements and regulatory networks. Journal of Experimental Botany 63:1593-1608. doi: 10.1093/jxb/err460, PMID: 22291134.
Pubmed: Author and Title
CrossRef: Author and Title
Google Scholar: Author Only Title Only Author and Title

Lin YF, Aarts MGM. 2012. The molecular mechanism of zinc and cadmium stress response in plants. Cell. Mol. Life Sci. 69:3187-3206. doi: 10.1007/s00018-012-1089-z, PMID: 22903262.
Pubmed: Author and Title
CrossRef: Author and Title
Google Scholar: Author Only Title Only Author and Title

Lipko A, Swiezewska E. 2016. Isoprenoid generating systems in plants — A handy toolbox how to assess contribution of the mevalonate and methylerythritol phosphate pathways to the biosynthetic process. Prog. Lipid Res. 63:70-92. doi: 10.1016/j.plipres.2016.04.002, PMID: 27133788.
Pubmed: Author and Title
CrossRef: Author and Title
Google Scholar: Author Only Title Only Author and Title

Mansouri H, Asrar Z, Mehrabani M. 2009. Effects of gibberellic acid on primary terpenoids and delta(9)-tetrahydrocannabinol in Cannabis sativa at flowering stage. J. Integ. Plant Biol. 51:553-561. doi: 10.1111/j.1744-7909.2009.00833.x, PMID: 19522814.
Pubmed: Author and Title
CrossRef: Author and Title
Google Scholar: Author Only Title Only Author and Title

Marquardt DW. 1963. An algorithm for least-squares estimation of nonlinear parameters. J. Soc. Industr. App. Mathem. 11:431-441.
Pubmed: Author and Title
CrossRef: Author and Title
Google Scholar: Author Only Title Only Author and Title

Maurel K, Sakr S, Gerbe F, Guilliot A, Bonhomme M, Rageau R, Pétel G. 2004. Sorbitol uptake is regulated by glucose through the hexokinase pathway in vegetative peach-tree buds. J. Exp. Bot. 55:879-888. doi: 10.1093/jxb/erh087, PMID: 14990620.
Pubmed: Author and Title
CrossRef: Author and Title
Google Scholar: Author Only Title Only Author and Title

May B, Lange BM, Wuest M. 2013. Biosynthesis of sesquiterpenes in grape berry exocarp of Vitis vinifera L.: Evidence for a transport of farnesyl diphosphate precursors from plastids to the cytosol. Phytochemistry 95:135-144. doi: 10.1016/j.phytochem.2013.07.021, PMID: 23954075.
Pubmed: Author and Title
CrossRef: Author and Title
Google Scholar: Author Only Title Only Author and Title

Meier S, Tzfadia O, Vallabhaneni R, Gehring C, Wurtzel ET. 2011. A transcriptional analysis of carotenoid, chlorophyll and plastidial isoprenoid biosynthesis genes during development and osmotic stress responses in Arabidopsis thaliana. BMC Systems Biol. 5:19. doi: 10.1186/1752-0509-5-77, PMID: 21595952.
Pubmed: Author and Title
CrossRef: Author and Title
Google Scholar: Author Only Title Only Author and Title

Meyer O, Hoeffler JF, Grosdemange-Billiard C, Rohmer M. 2004. Practical synthesis of 1-deoxy-D- xylulose and 1-deoxy-d-xylulose 5-phosphate allowing deuterium labeling. Tetrahedron; 60:12153-12162. doi:10.1016/j.tet.2004.10.016.
Pubmed: Author and Title
CrossRef: Author and Title
Google Scholar: Author Only Title Only Author and Title

Moremen KW, Tiemeyer M, Nairn AV. 2012. Vertebrate protein glycosylation: diversity, synthesis and function. Nat. Rev. Mol. Cell Biol. 13:448-462. PMID: 22722607.
Pubmed: Author and Title
CrossRef: Author and Title
Google Scholar: Author Only Title Only Author and Title

Moreno AA, Orellana A. 2011. The physiological role of the unfolded protein response in plants. Biol. Res. 44:75-80. doi: 10.4067/S0716-97602011000100010, PMID: 21720684.
Pubmed: Author and Title
CrossRef: Author and Title
Google Scholar: Author Only Title Only Author and Title

Nagegowda DA, Ramalingam S, Hemmerlin A, Bach TJ, Chye ML. 2005. Brassica juncea HMG-CoA synthase: localization of mRNA and protein. Planta 221:844-856. doi: 10.1007/s00425-005-1497-5, PMID: 15770484.
Pubmed: Author and Title
CrossRef: Author and Title
Google Scholar: Author Only Title Only Author and Title

Obata T, Fernie AR. 2012. The use of metabolomics to dissect plant responses to abiotic stresses. Cell. Mol. Life Sci. 69:3225-3243. doi: 10.1007/s00018-012-1091-5, PMID: 22885821.
Pubmed: Author and Title
CrossRef: Author and Title
Google Scholar: Author Only Title Only Author and Title

Opitz S, Nes WD, Gershenzon J. 2014. Both methylerythritol phosphate and mevalonate pathways contribute to biosynthesis of each of the major isoprenoid classes in young cotton seedlings. Phytochemistry 98:110-119. doi: 10.1016/j.phytochem.2013.11.010, PMID: 24359633.
Pubmed: Author and Title
CrossRef: Author and Title
Google Scholar: Author Only Title Only Author and Title

Pokhilko A, Bou-Torrent J, Pulido P, Rodríguez-Concepción M, Ebenhöh O. 2015. Mathematical modelling of the diurnal regulation of the MEP pathway in Arabidopsis. New Phytol. 206:1075-1085. doi: 10.1111/nph.13258. PMID: 25598499.
Pubmed: Author and Title
CrossRef: Author and Title
Google Scholar: Author Only Title Only Author and Title

Pulido P, Perello C, Rodriguez-Concepcion M. 2012. New insights into plant isoprenoid metabolism. Mol. Plant 5:964-967. doi: 10.1093/mp/sss088, PMID: 22972017.
Pubmed: Author and Title
CrossRef: Author and Title
Google Scholar: Author Only Title Only Author and Title

Rohmer M. 1999. The discovery of a mevalonate-independent pathway for isoprenoid biosynthesis in bacteria, algae and higher plants. Nat. Prod. Rep. 16:565-574. PMID: 10584331.
Pubmed: Author and Title
CrossRef: Author and Title
Google Scholar: Author Only Title Only Author and Title

Schenk B, Rush JS, Waechter CJ, Aebi M. 2001. An alternative cis-isoprenyltransferase activity in yeast that produces polyisoprenols with chain lengths similar to mammalian dolichols. Glycobiology 11:89-98. PMID: 11181565.
Pubmed: Author and Title
CrossRef: Author and Title
Google Scholar: Author Only Title Only Author and Title

Schuhr CA, Radykevicz T, Sagner S, Latzel C, Zenk MH, Arigoni D, Bacher A, Rohdich F, Eisenreich W. 2003. Quantitative assessment of metabolite flux by NMR spectroscopy. Crosstalk between the two isoprenoid biosynthesis pathways in plants. Phytochem. Rev. 2:3-16. doi: 10.1023/B:PHYT.0000004180.25066.62.
Pubmed: Author and Title
CrossRef: Author and Title
Google Scholar: Author Only Title Only Author and Title

Schwarz F, Aebi M. 2011. Mechanisms and principles of N-linked protein glycosylation. Curr. Opin. Struct. Biol. 21:576-582. PMID: 21978957.
Pubmed: Author and Title
CrossRef: Author and Title
Google Scholar: Author Only Title Only Author and Title

Selmar D, Kleinwaechter M. 2013. Stress enhances the synthesis of secondary plant products: the impact of stress-related over-reduction on the accumulation of natural products. Plant Cell Physiol. 54:817-826. doi: 10.1093/pcp/pct054, PMID: 23612932.
Pubmed: Author and Title
CrossRef: Author and Title
Google Scholar: Author Only Title Only Author and Title

Shai N, Schuldiner M, Zalckvar E. 2016. No peroxisome is an island - Peroxisome contact sites. Biochim. Bophys. Acta 1863:1061-1069. doi: 10.1016/j.bbamcr.2015.09.016, PMID: 26384874.
Pubmed: Author and Title
CrossRef: Author and Title
Google Scholar: Author Only Title Only Author and Title

Sharma R, De Vleesschauwer D, Sharma MK, Ronald PC. 2013. Recent advances in dissecting stress-regulatory crosstalk in rice. Mol. Plant 6:250-260. doi: 10.1093/mp/sss147, PMID: 23292878.
Pubmed: Author and Title
CrossRef: Author and Title
Google Scholar: Author Only Title Only Author and Title

Simkin AJ, Guirimand G, Papon N, Courdavault V, Thabet I, Ginis O, Bouzid S, Giglioli-Guivarc'h N, Clastre M. 2011. Peroxisomal localisation of the final steps of the mevalonic acid pathway in planta. Planta 234:903-914. doi: 10.1007/s00425-011-1444-6, PMID: 21655959.
Pubmed: Author and Title
CrossRef: Author and Title
Google Scholar: Author Only Title Only Author and Title

Skoneczny M, Kludkiewicz B, Swiezewska E, Szkopinska A. 2006. Activity of Pichia pastoris alternative cis-prenyltransferase is correlated with proliferation of peroxisomes. Cell Biol. Int. 30:122-6. doi: 10.1016/j.cellbi.2005.09.006, PMID: 16271301.
Pubmed: Author and Title
CrossRef: Author and Title
Google Scholar: Author Only Title Only Author and Title

Skorupinska-Tudek K, Bienkowski T, Olszowska O, Furmanowa M, Chojnacki T, Danikiewicz W, Swiezewska E. 2003. Divergent pattern of polyisoprenoid alcohols in the tissues of Coluria geoides: a new electrospray ionization MS approach. Lipids. 38:981-90. PMID: 14584606.
Pubmed: Author and Title
CrossRef: Author and Title
Google Scholar: Author Only Title Only Author and Title

Skorupinska-Tudek K, Poznanski J, Wojcik J, Bienkowski T, Szostkiewicz I, Zelman-Femiak M, Bajda A, Chojnacki T, Olszowska O, Grunler J, Meyer O, Rohmer M, Danikiewicz W, Swiezewska E. 2008. Contribution of the mevalonate and methylerythritol phosphate pathways to the biosynthesis of dolichols in plants. J. Biol. Chem. 283:21024-21035. doi: 10.1074/jbc.M706069200, PMID: 18502754.
Pubmed: Author and Title
CrossRef: Author and Title
Google Scholar: Author Only Title Only Author and Title

Strasser R. 2016. Plant protein glycosylation. Glycobiology 26:926-939. doi: 10.1093/glycob/cww023, PMID: 26911286.
Pubmed: Author and Title
CrossRef: Author and Title
Google Scholar: Author Only Title Only Author and Title

Surmacz L, Plochocka D, Kania M, Danikiewicz W, Swiezewska E. 2014. cis-Prenyltransferase AtCPT6 produces a family of very short-chain polyisoprenoids in planta. Biochim. Biophys. Acta 1841:240-250. doi: 10.1016/j.bbalip.2013.11.011, PMID: 24291644.
Pubmed: Author and Title
CrossRef: Author and Title
Google Scholar: Author Only Title Only Author and Title

Surmacz L, Swiezewska E. 2011. Polyisoprenoids - Secondary metabolites or physiologically important superlipids? Biochem. Biophys. Res. Comm. 407:627-632. doi: 10.1016/j.bbrc.2011.03.059, PMID: 21419101.
Pubmed: Author and Title
CrossRef: Author and Title

Google Scholar: Author Only Title Only Author and Title

Swiezewska E, Danikiewicz W. 2005. Polyisoprenoids: structure, biosynthesis and function. Prog. Lipid Res. 44:235-258. PMID: 16019076.
Pubmed: Author and Title
CrossRef: Author and Title
Google Scholar: Author Only Title Only Author and Title

Thompson SL, Burrows R, Laub RJ, Krisans SK. 1987. Cholesterol synthesis in rat liver peroxisomes. Conversion of mevalonic acid to cholesterol. J. Biol. Chem. 262:17420-17425. PMID: 3693362.
Pubmed: Author and Title
CrossRef: Author and Title
Google Scholar: Author Only Title Only Author and Title

Valentovic P, Luxova M, Kolarovic L, Gasparikova O. 2006. Effect of osmotic stress on compatible solutes content, membrane stability and water relations in two maize cultivars. Plant Soil Envir. 52:186-191.
Pubmed: Author and Title
CrossRef: Author and Title
Google Scholar: Author Only Title Only Author and Title

Walley J, Xiao Y, Wang JZ, Baidoo EE, Keasling JD, Shen Z, Briggs SP, Dehesh K. 2015. Plastid-produced interorgannellar stress signal MEcPP potentiates induction of the unfolded protein response in endoplasmic reticulum. Proc. Natl Acad. Sci. USA 112:6212-6217. doi: 10.1073/pnas.1504828112, PMID: 25922532.
Pubmed: Author and Title
CrossRef: Author and Title
Google Scholar: Author Only Title Only Author and Title

Wu SJ, Shi M, Wu JY. 2009. Cloning and characterization of the 1-deoxy-D-xylulose 5-phosphate reductoisomerase gene for diterpenoid tanshinone biosynthesis in Salvia miltiorrhiza (Chinese sage) hairy roots. Biotech. Appl. Biochem. 52:89-95. doi: 10.1042/BA20080004, PMID: 18302535.
Pubmed: Author and Title
CrossRef: Author and Title
Google Scholar: Author Only Title Only Author and Title

Xiao Y, Savchenko T, Baidoo EE, Chehab WE, Hayden DM, Tolstikov V, Corwin JA, Kliebenstein DJ, Keasling JD, Dehesh K. 2012. Retrograde signaling by the plastidial metabolite MEcPP regulates expression of nuclear stress-response genes. Cell 149:1525-1535. doi: 10.1016/j.cell.2012.04.038, PMID: 22726439.
Pubmed: Author and Title
CrossRef: Author and Title
Google Scholar: Author Only Title Only Author and Title

Yan X, Zhang L, Wang J, Liao P, Zhang Y, Zhang R, Kai G. 2009. Molecular characterization and expression of 1-deoxy-d-xylulose 5-phosphate reductoisomerase (DXR) gene from Salvia miltiorrhiza. Acta Phys. Plant. 31:1015-1022. doi:10.1007/s11738-009-0320-5.
Pubmed: Author and Title
CrossRef: Author and Title
Google Scholar: Author Only Title Only Author and Title

Yang D, Du X, Liang X, Han R, Liang Z, Liu Y, Liu F, Zhao J. 2012. Different roles of the mevalonate and methylerythritol phosphate pathways in cell growth and tanshinone production of Salvia miltiorrhiza hairy roots. Plos One 7:e46797. doi: 10.1371/journal.pone.0046797, PMID: 23209548.
Pubmed: Author and Title
CrossRef: Author and Title
Google Scholar: Author Only Title Only Author and Title